

**Design and Analysis of an Embedded Pipe Network in Asphalt Pavements to Reduce  
the Urban Heat Island Effect**

by

Jonathan J. Carelli

A Thesis

Submitted to the Faculty

of the

WORCESTER POLYTECHNIC INSTITUTE

in partial fulfillment of the requirements for the

Degree of Master of Science

in

Civil Engineering

May 2010

APPROVED:



Dr. Rajib B. Mallick  
WPI, Major Advisor



Dr. Leonard D. Albano  
WPI, Advisor



Dr. Tahar El-Korchi  
WPI, Department Head

## **Abstract**

Urban areas contain significant amounts of asphalt pavement. When exposed to the sun, asphalt pavement absorbs solar radiation and stores it as thermal energy raising its temperature. According to the urban heat island effect (UHIE), the pavement releases the thermal energy back to the surrounding air resulting in a rise in local air temperature. A pipe network containing a passing fluid installed in the pavement can reduce the UHIE. The fluid captures the thermal energy stored in the pavement, reducing air and pavement temperatures as well as providing heated water for other applications. The heat transfer/harvesting system can be optimized to produce the desired cooling of the pavements. This research addresses the economic feasibility of a pipe network by design as well as structural performance through computer modeling. To design the pipe network and predict its economic feasibility an Excel spreadsheet was programmed. It requires local air temperature data to determine the yearly temperature profile within the pavement and to calculate the amount of thermal energy that could be extracted. By varying design parameters such as fluid flow rate, it produces a matrix of payback periods. Structural conditions were considered for the installation of the proposed system. To simultaneously evaluate the thermal and structural performance of the pipe network installation, a finite element model was created using COMSOL Multiphysics©. A typical value of solar radiation and a standard truck tire wheel load were applied to the model to simulate the intended application of the pipe network. The result of this thesis is a method and a tool to design and analyze with respect to economic and structural performance a pipe network used to extract the thermal energy stored in asphalt pavements and reduce the UHIE.

## Table of Contents

Abstract.....	i
1. Introduction.....	1
2. Background.....	3
2.1. Urban Heat Island Effect (UHIE) and the Proposed Solution.....	3
2.2. Heat Transfer.....	5
2.3. Field Experiments.....	7
2.4. Comparison of FEM and Field Experiments.....	11
3. Methodology.....	13
3.1. Material Properties.....	13
3.2. Economic Analysis.....	18
3.3. Computer Modeling.....	26
4. Results.....	29
4.1. Economic Analysis.....	29
4.2. Computer Modeling.....	33
4.2.1. Study One: Constant vs. Varying Poisson's Ratio.....	35
4.2.2. Study Two: Stress vs. Pipe Depth.....	37
4.2.3. Study Three: Stress vs. Temperature for Different Pipe Materials.....	38
5. Conclusions and Recommendations.....	41
References.....	45
Appendix A: Example Economic Analysis (Houston, Texas).....	47
Appendix B: Study One: Constant vs. Varying Poisson's Ratio.....	62

## List of Figures

Figure 1: Proposed solution concept (Mallick et al., 2009) .....	4
Figure 2: Maximum pavement temperature vs. pavement service life (Chen, 2008) .....	5
Figure 3: Experimental schematic.....	8
Figure 4: Outdoor experimental setup .....	8
Figure 5: Typical experimental result (with solar exposure).....	9
Figure 6: Typical experimental result (with water $\Delta T$ ) .....	10
Figure 7: Proposed solution (left) Experimental slab (middle), FE Model, (right) FE solution (Chen, 2008).....	11
Figure 8: Comparison of experimental and FEM temperature results (left) surface (right) .....	12
Figure 9: Pipe material versus water outlet temperature .....	15
Figure 10: Temperature profile for 24-hour period containing the maximum pavement temperature (Houston, TX) (0, 1, 2, 3, 4, 5, 6 inch pavement depths) .....	22
Figure 11: COMSOL model dimensions (length into page).....	26
Figure 12: One-year pavement temperature profiles: (1) Phoenix, AZ (2) Houston, TX (3) Miami, FL (4) Boston, MA .....	30
Figure 13: Example thermal solution (left) before water flow, (right) after flow .....	33
Figure 14: Example structural solution (left) pipe stresses, (right) pavement stresses.....	34
Figure 15: Points of investigation for critical stresses .....	35
Figure 16: Constant vs. varying Poisson's Ratio (2" pipe depth) (top) copper pipe (bottom) HMA.....	37
Figure 17: Stress vs. pipe depth .....	38
Figure 18: Stress vs. temperature for copper, PVC, and PEX (4" pipe depth) .....	40
Figure 19: Example 'Input' worksheet.....	47
Figure 20: Example 'Statistics' worksheet (continued on following pages) .....	48
Figure 21: Example 'Profile' worksheet .....	52
Figure 22: Example 'Profile Summary' Worksheet (continued on the next page) .....	53
Figure 23: Example 'Results' worksheet (continued on the next page) .....	55
Figure 24: Constant vs. varying Poisson's Ratio (2" pipe depth) (top) copper pipe (bottom) HMA.....	62
Figure 25: Constant vs. varying Poisson's Ratio (4" pipe depth) (top) copper pipe (bottom) HMA.....	63
Figure 26: Constant vs. varying Poisson's Ratio (6" pipe depth) (top) copper pipe (bottom) HMA.....	64

## List of Tables

Table 1: Summary of thermal material properties .....	14
Table 2: Summary of structural material properties .....	16
Table 3: Economic analysis summary .....	32
Table 4: Stress summary .....	40

## **1. Introduction**

Urban areas contain significant amounts of impervious surface in the form of parking lots and roads consisting of asphalt pavement. During the day these surfaces are exposed to significant amounts of solar radiation. The solar radiation is absorbed by the asphalt pavement and converted into thermal energy to be stored within the pavement. The thermal energy is then released back to the environment causing a local rise in air temperature in what is known as the urban heat island effect (UHIE). This phenomenon continues after sunset allowing urban areas to maintain an air temperature greater than that present in the surrounding rural areas. One undesired effect of the urban heat island effect is an increase the amount of energy required to cool the surrounding structures due to the increase in external ambient air temperature.

While asphalt pavements influence the local environment through the UHIE they also provide a tremendous environmental opportunity. The thermal energy stored within in the pavement can be harnessed for a wide variety of applications from use in heat exchangers to power generation. By harnessing the energy stored in the pavement, less is released back to the environment thus reducing the UHIE. A local reduction in air temperature achieves additional benefits such as a reduced demand from local buildings for energy for cooling.

A solution based on the concept of the solar hot water panel has been developed to harness the available thermal energy. Field experiments and computer modeling support the conceptual feasibility of the proposed solution and the ability to effectively model the heat transfer phenomenon using finite element software. Conceptual feasibility alone, however, does not result in immediate widespread implementation of the proposed

solution. Economic feasibility must be established to make investment appealing and structural survivability must be determined to ensure that in installation will last.

This thesis first addresses the next logical step towards implementation of the proposed solution which is the determination of the economic feasibility. A programmed spreadsheet assists in the evaluation of the economic feasibility of the proposed solution at a given location. In doing so a matrix of system parameters are evaluated to provide many design alternatives for which the payback period is determined for that location. Locations closer to the equator which have high ambient temperatures serve as the most economically feasible locations.

This thesis lastly begins to address the concept of structural survivability of the proposed solution whereby the materials used and their interactions are investigated through computer modeling. The result of this thesis is a process by which the economic feasibility for a location can be established through the use of a programmed allowing for selection of design parameters to input into a corresponding computer model.

Background information on the proposed solution, the urban heat island effect and heat transfer principles will be discussed. The results of field experiments and preliminary computer modeling will establish conceptual feasibility of the proposed solution. Utilization of a spreadsheet programmed to predict pavement temperature will assist in establishing economic feasibility and provide design options. Further computer modeling with appropriate material properties will establish structural survivability of the proposed solution.

## **2. Background**

In order to develop a method for which to design and analyze a system to extract the thermal energy from pavements several topics must be addressed. First, the proposed solution concept must be completely described. Next, the applicable heat transfer principles must be discussed to understand the energy path from the sun to the passing fluid. Field experiments support the conceptual feasibility of the proposed solution providing a measurable reduction in pavement temperature and increase in water temperature. Agreement between experimental results and computer modeling results support further studies of the proposed solution using the same computer software.

### **2.1. Urban Heat Island Effect (UHIE) and the Proposed Solution**

Asphalt pavements when exposed to the sun, absorb the solar radiation and convert it to thermal energy that is stored within the pavement. The pavement then releases this thermal energy back to the environment increasing the local ambient air temperature. In larger scale, as witnessed in urban areas where there are significant amounts of impervious surfaces due to roads and parking lots, this phenomenon is known as the urban heat island effect (UHIE). One solution to harness the stored thermal energy and reduce the UHIE is to place a pipe within the pavement and flow an appropriate fluid through the pipe as diagrammed in Figure 1.

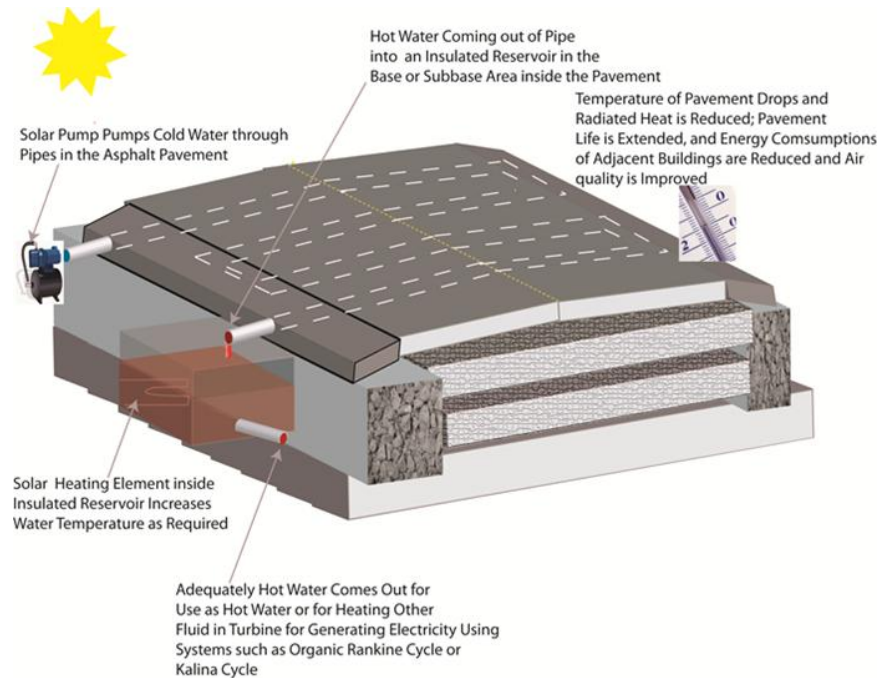


Figure 1: Proposed solution concept (Mallick et al., 2009)

The pavement at a higher temperature passes the heat to the cooler fluid increasing the temperature of the fluid and decreasing the temperature of the pavement. The length and flow rate through the pipe network can be established to yield a heated fluid at a temperature equal to the temperature of the pavement at the depth of the pipe network. The heated fluid may be used to generate electricity, used simply as heated water, or stored for later use such as to heat the road surface. By reducing the temperature of the pavement, less heat is released back to the environment thus reducing the UHIE.

Implementation of the proposed solution has additional benefits including a reduced cooling load for the buildings immediately surrounding the pavement. Less energy is then consumed from the electricity grid to cool the building. A reduction in the pavement temperature also increases expected pavement service life as shown in Figure 2. In example, if the maximum pavement temperature experienced during the year is reduced from 70 degrees Celsius to 63 degrees Celsius, the pavement may last up to 5 additional

year before needing repairs. The temperature reduction increases the stiffness of the pavement resulting in a greater resistance against rutting.

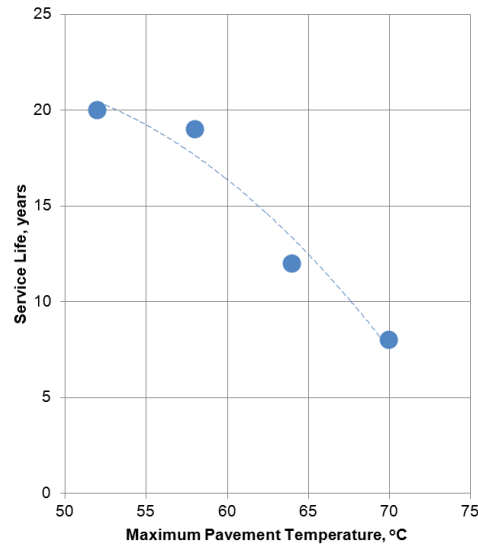


Figure 2: Maximum pavement temperature vs. pavement service life (Chen, 2008)

## 2.2. Heat Transfer

Heat transfer is the principal mechanism behind both the urban heat island effect as well as the proposed solution to reduce its effects. The sun provides a continuous source of radiation to which the surface of the asphalt pavement is exposed. The fraction of the incident radiation that is absorbed by the asphalt is dictated by the material's emissivity,  $\epsilon$ . The remaining fraction reflects off the surface back to the surrounding air and other surfaces. As a result of absorption the pavement surface temperature begins to increase as the solar energy is converted to thermal energy stored within the pavement.

The thermal energy flows deeper into the pavement through conduction which requires the direct contact of the molecules of the material increasing the temperature at depth. The material property that dictates how readily this heat flows through the material is its thermal conductivity,  $k$ . The higher the thermal conductivity, the more readily heat

flows through the material. Another material property, specific heat capacity,  $c$ , defines that amount of energy required to raise a specific mass of that material by one degree in temperature. A material of a higher specific heat capacity requires more energy to heat the material by the same temperature amount and provides greater storage of energy.

The stored thermal energy flows through the thickness of the pipe by conduction and to the fluid by convection. The rate of flow to the fluid depends on the thermal conductivity of the fluid,  $k$ , the flow rate of the fluid,  $Q$ , and the initial temperature of the fluid. An increased flow rate supports quicker flow of energy from the surroundings with which it is in contact.

Loomans et al. (2003) has developed a three segment model to mathematically evaluate the proposed solution concept. The top segment considers the incident solar radiation, the radiation loss to the sky, the conduction to the lower layers of the pavement, and the convective heat loss from the surface due to natural convection and wind. The middle segment accounts for the convective loss of heat from the pavement due to the passing fluid. The lower segment represents conduction of heat through the layers of pavement and subgrade below the depth of the pipe network. Conduction of heat through the pipe walls is not addressed in this model separately as it may

The UHIE is the result of convective and radiative heat losses from the surface of the pavement. The rate convective heat loss is defined by a convective heat loss coefficient,  $h$ , which is difficult to determine as it encompasses the properties of the material and the fluid as well as the geometrical relation between the two. Factors such as local wind speed affect the value of the heat transfer coefficient. Radiative heat loss is a function of the emissivity of the surface material,  $\epsilon$ , the Stefan-Boltzman constant,  $\sigma$ , taken as  $5.68 \times 10^{-8}$

W/(m<sup>2</sup>K<sup>4</sup>), and the temperatures of the surface and ambient fluid according to the following formula:

$$q_{released} = \varepsilon\sigma(T_{pavement}^4 - T_{ambient}^4) \quad (1)$$

The radiative heat released is a function of the surface temperature of the pavement to the fourth power. A small reduction in pavement temperature thus significantly reduces the amount of heat released back to the environment. Although the pipe network is at a depth within the pavement, the flowing fluid reduces the surface temperature after sufficient time has passed. The proposed solution reduces the overall temperature of the pavement including the surface thus reducing the UHIE.

### **2.3. Field Experiments**

In order to establish the conceptual feasibility of the proposed solutions field experiments must be conducted. The goal of these experiments is to show that passing a fluid (water) through a slab of asphalt pavement reduces the temperature of the pavement at the surface and at depth as well as results in a significant rise in the temperature of the water. Reduction in the pavement temperature addresses the desire to reduce the urban heat island effect. A rise in fluid temperature signifies economic advantage of the proposed solution due to its many applications.

Figure 3 presents an experimental schematic for the investigation an asphalt pavement slab. To appropriately study the phenomenon, the experimental setup must be placed outside for exposure to the sun as shown in Figure 4. In this experiment, the pavement is exposed to the sun for a period of two hours from approximately 10 AM to 12 noon to allow the pavement to heat. At this time, the fluid begins to flow and continues to

do so for four hours until 4 PM at which point the experiment is terminated. The experiment must be repeated several times to establish the repeatability of the concept.

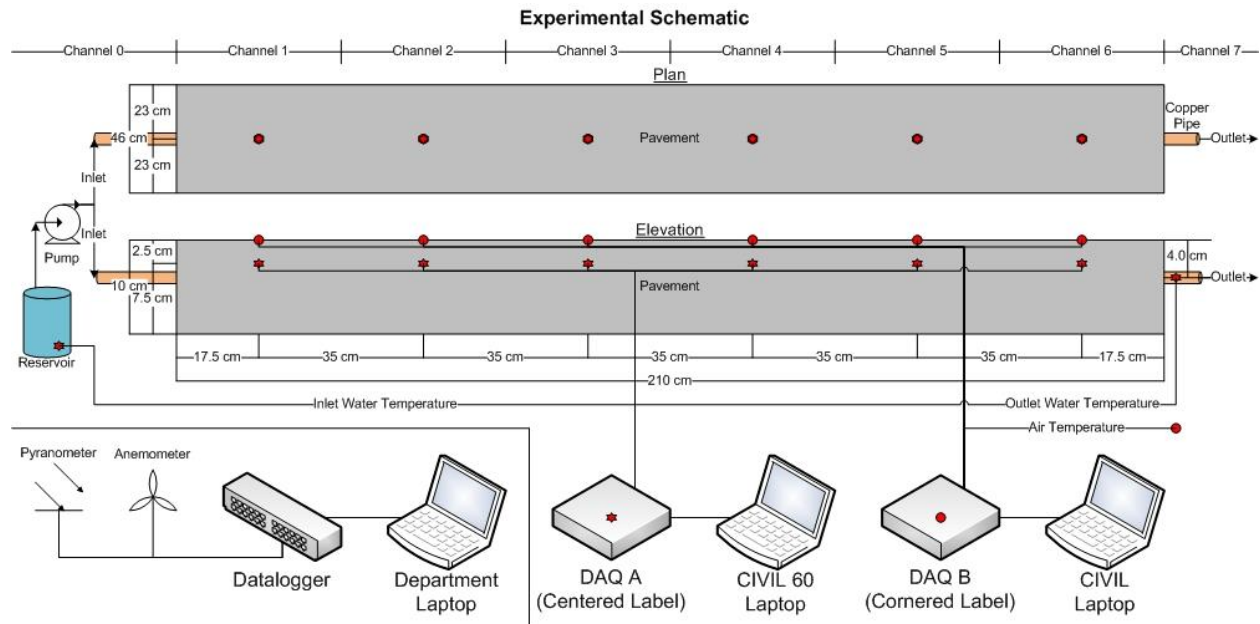


Figure 3: Experimental schematic



Figure 4: Outdoor experimental setup

During the experiment, measurements of the temperature of the pavement using thermocouples are taken at five different locations evenly spaced along the surface and at a depth of 25 mm (1 inch). Additional thermocouples measure the temperature of the inlet and outlet water temperature as well as the ambient air

temperature. An anemometer measures the wind speed and a pyranometer measure the incident solar radiation at the location to determine the magnitude of solar exposure.

Figure 5 presents results from this experiment providing the air temperature, asphalt surface temperature, and asphalt temperature at depth (25 mm (1 inch)) as a function of time (in minutes) during the experiment. The temperature at the pavement surface and at depth represent an average of the five thermocouples at that depth. Figure 5 identifies a peak solar exposure of approximately 1100 W/m<sup>2</sup> at the experiment location Worcester, Massachusetts.

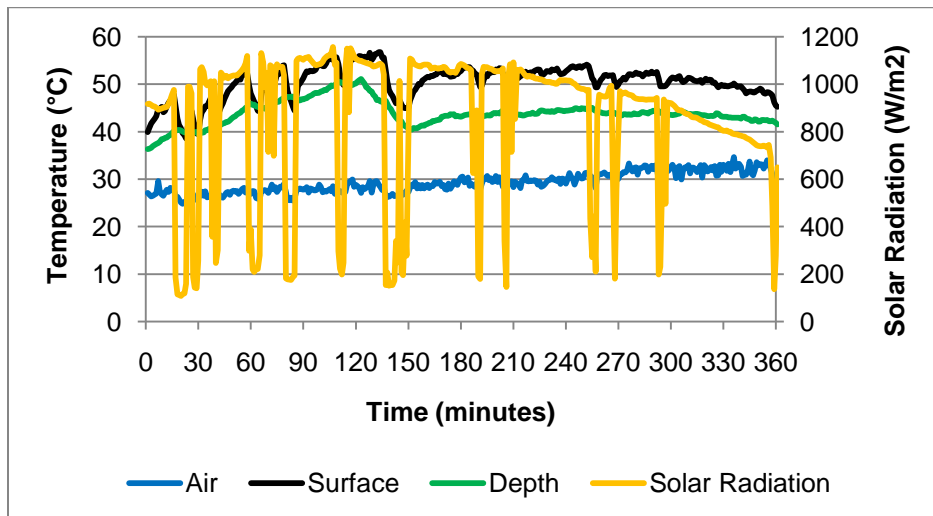


Figure 5: Typical experimental result (with solar exposure)

Figure 6 presents the surface, depth, and air temperature as provided in Figure 5 but with the addition of the difference in temperature,  $\Delta T$ , of the water measured at the inlet and the outlet of the asphalt slab. Figure 6 shows that at the start of the flow of water at 120 minutes into the experiment, the temperature at the surface and at depth drops approximately 10 Celsius degrees. The temperature at the surface falls quicker due to the cloudy moment occurring at the same time as indicated by a reduced solar exposure in Figure 5. Upon recession of the clouds, the pavement begins to heat but maintains a

temperature lower than before the start of the flow suggesting a permanent decrease in the surface temperature. At depth, the difference in pavement temperature before and after the start of the flow of water is more pronounced suggesting successful extraction by the passing water. The difference in surface temperature achieves the goal of reducing the urban heat island effect.

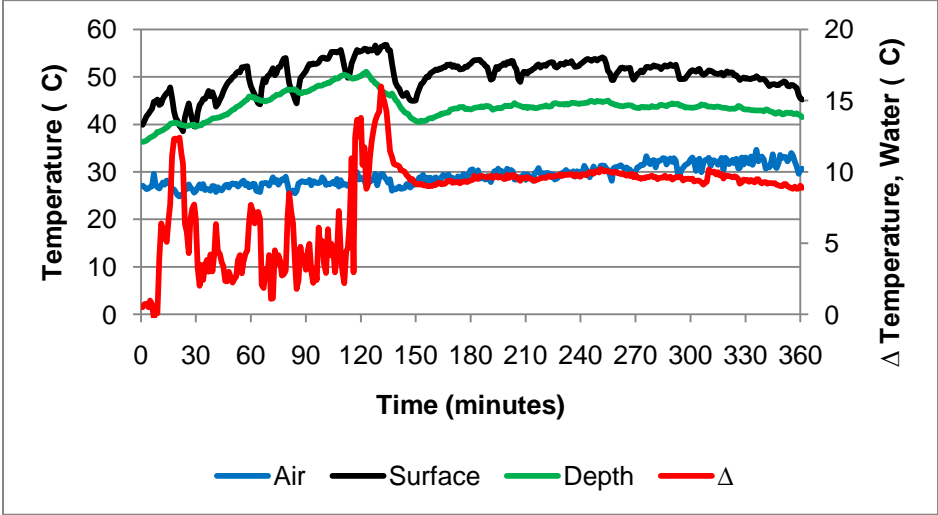


Figure 6: Typical experimental result (with water  $\Delta T$ )

At the start of the flow of water, the water exits the pipe at an increased temperature due to its greater contact time and/or existence in the pipe prior to the initiation of flow. Once the flow reaches steady state after about 30 minutes the temperature of the water at the outlet measures consistently around 9 Celsius degrees greater than the input temperature. This change in temperature is a measure of the amount of thermal energy extracted from the pavement. The magnitude of temperature difference over the small distance of 210 centimeters (83 inches) suggests that a longer embedded pipe distance could yield a greater temperature difference and thus more energy harvested from the pavement. This results in a greater economic advantage. Such field experiments establish conceptual feasibility by lowering the surface temperature of

the pavement reducing the urban heat island effect as well as providing an economic advantage and extra incentive through the significant heating of the water over a short length of embedded pipe.

## 2.4. Comparison of FEM and Field Experiments

Finite element (FE) software allows the investigation of a problem without the need to construct an actual experiment. As such, it is also especially effective at investigating changes in parameter to investigate the sensitivity of such parameters without the need to construct additional experiments. A model is designed in the software as if it were a field experiment including the appropriate dimensions, material properties, and environmental conditions. One particular finite element software, COMSOL Multiphysics®, allows the coupling of different phenomena such as heat transfer, and structural mechanics to investigate their inter-relationship (COMSOL Multiphysics®, 2008). To determine the ability to effectively model the proposed solution in the COMSOL software, Chen first conducted a field experiment similar to that outlined in Section 2.3 with a larger slab and more pipes arranged as shown in Figure 7.

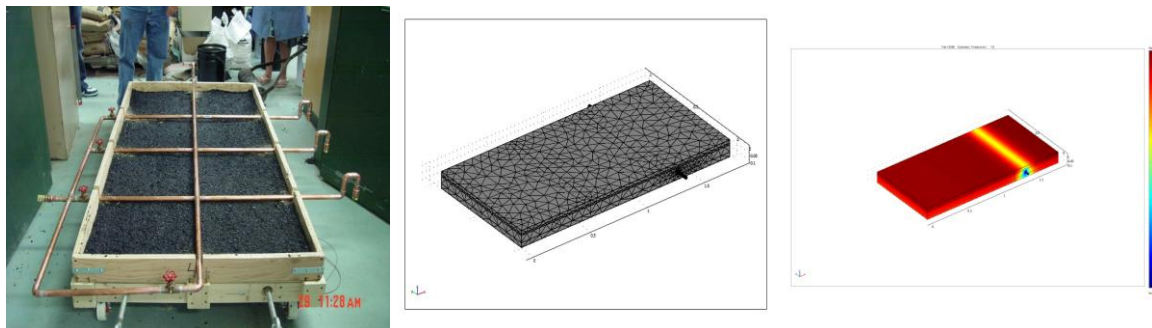


Figure 7: Proposed solution (left) Experimental slab (middle), FE Model, (right) FE solution (Chen, 2008)

Chen then constructed a finite element model also shown in Figure 7 to match the experimental slab but only including a single pipe near to the edge of slab. Appropriate

thermal material properties were applied as well as thermal boundary conditions and the model is solved. Points of temperature comparison were chosen to be at the surface and at a depth of one inch below the surface aligned with the center of the pipe. Then compared the temperatures obtained in the field experiment with those obtained from the finite element as presented in Figure 8. This closeness of the field experiment and finite element model temperatures suggests that COMSOL Multiphysics© can reliably model the thermal behavior of the proposed solution. This confirmation allows the conduction of other studies under the expectation that the results will be correct.

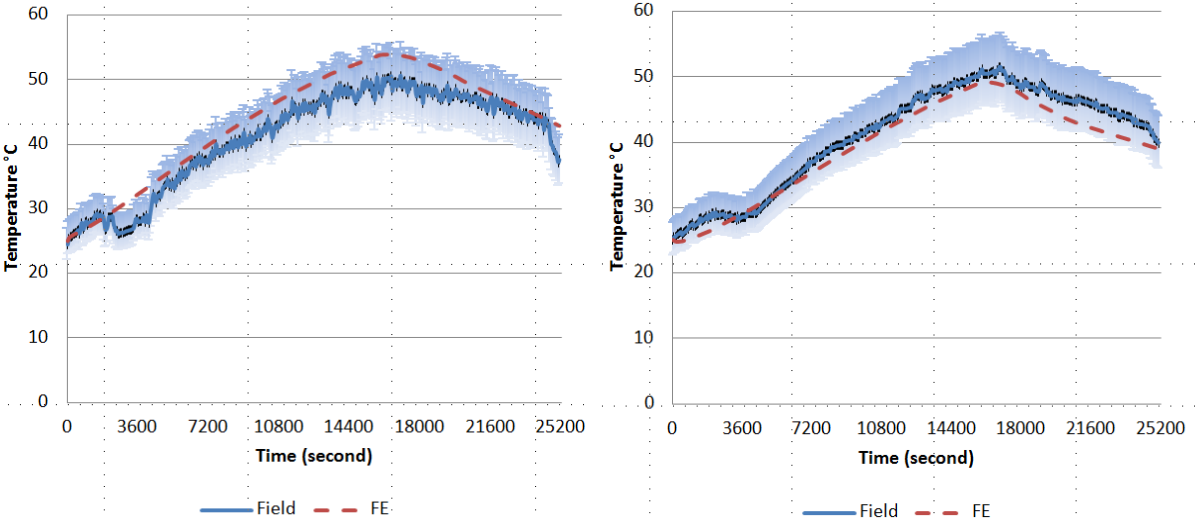


Figure 8: Comparison of experimental and FEM temperature results (left) surface (right) (1" depth)

### **3. Methodology**

With the conceptual feasibility of the proposed solution established both economic feasibility and structural survivability can be investigated. Material properties influence both the economic feasibility and the structural survivability of the proposed solution. To determine the economic feasibility at a location, a spreadsheet was programmed that accepts local environmental parameters as well as material properties and associated costs for the installation and maintenance of the system. From the output of this spreadsheet a design may be chosen for which an equivalent computer model can be created in COMSOL. In this model, the thermal performance of the design can be verified as well as structural survivability when subjected to conditions expected at its installation location.

#### **3.1. Material Properties**

Material properties play an essential role in both the thermal and structural behavior of the proposed solution. The economic feasibility of the proposed solution is based upon the high specific heat capacity of the asphalt pavement as well as its low thermal conductivity. The high specific heat capacity allows the pavement to store significant amounts of energy for a finite temperature increase and the low thermal conductivity slows the travel of the heat through the depth of the pavement. The amount of the solar radiation which an asphalt pavement absorbs is a function of the material's emissivity. Loomans et al. (2003) specifies a range of 0.88 to 0.93 for the emissivity of fresh asphalt pavements which indicates that the pavement absorbs nearly 90 percent of the solar radiation to which it is exposed. A perfect black-body which absorbs all of the incident radiation to which it is exposed has an emissivity of 1. The age of the asphalt can cause a decrease in this value.

Table 1 contains a summary of the thermal properties of each of the materials investigated during computer modeling.

Table 1: Summary of thermal material properties

<b>Material</b>	<b>k (W/m*K)</b>	<b><math>\rho</math> (kg/m<sup>3</sup>)</b>	<b>Cp (J/kg*K)</b>
<b>HMA</b>	1.8	2350	1050
<b>Air</b>	0.026	1.1843	1006.25
<b>Water</b>	0.6	1000	4186
<b>Copper</b>	400	8700	385
<b>Aluminum</b>	160	2700	900
<b>Iron</b>	76.2	7870	440
<b>Nylon</b>	0.26	1150	1700
<b>PEX</b>	0.41	935	2100

The material properties of the pipe are of concern when modeling the performance of the proposed solution. The pipe material must be of high thermal conductivity to provide a quick path for the energy to flow from the surrounding pavement to the passing fluid. Figure 9 presents the results of a study to determine the effect of the pipe material on the outlet temperature of the continuously flowing water within the pavement. There is little difference between the copper, aluminum, and iron, but a significant decrease in the outlet temperature when the material is nylon. This is due to the low thermal conductivity of the material where the stored thermal energy passes more slowly to the flowing water. In practice, this would require the installation of a much greater length of pipe to achieve an outlet water temperature equal to the temperature of the pavement. While the material, nylon, may not be used directly as the pipe material in the field, the thermal behavior of a material of a similar thermal conductivity can be predicted.

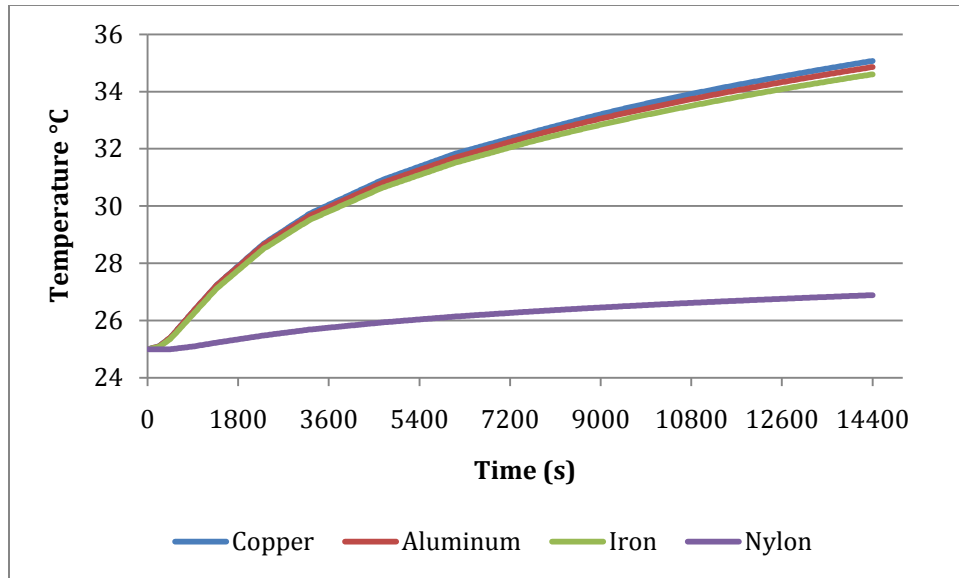


Figure 9: Pipe material versus water outlet temperature

Material properties are equally important in the determination of the structural survivability of the proposed solution. Three structural properties are required for proper computer modeling: modulus of elasticity, Poisson's ratio, and the thermal coefficient of expansion. The modulus of elasticity,  $E$ , is a property that defines the stiffness of a material indicating the level of strain for a given level of stress. Poisson's ratio,  $\nu$ , dictates the fraction of the stresses which are translated into different axes. Lastly, the thermal coefficient of expansion,  $\alpha$ , defines an amount of strain produced in the material per each degree change in temperature. Another material property not used directly in the computer modeling but critical in establishing structural survivability is the yield strength,  $F_y$ , of a material is an upper limit on the allowable stress to be present in the material under load after which the material begins to deform plastically which is not recoverable. Stress levels below this value result in the elastic return of the material to its original geometry after the load is removed. Materials containing stresses less than its yield strength under

loading have achieved structural survivability. Table 2 contains these structural material properties for each of the materials examined through computer modeling.

Table 2: Summary of structural material properties

<b>Material Property</b>	<b>Material</b>			
	<b>HMA</b>	<b>Copper</b>	<b>PVC</b>	<b>PEX</b>
<b>Modulus of Elasticity, E (psi)</b>	Variable	Variable	420,000	91,400
<b>Poisson's Ratio, <math>\nu</math></b>	Variable	0.35	0.41	0.41
<b>Coefficient of Thermal Expansion, <math>\alpha</math> (1/K)</b>	2.63E-05	1.69E-05	5.22E-05	4.32E-05
<b>Yield Strength, <math>F_y</math> (psi)</b>	300	50,000	7450	2180

Hot mix asphalt is a thermoplastic material meaning that its structural material properties vary greatly with changes in temperature. As such, its modulus of elasticity and Poisson ratio is listed as variable in Table 2. To properly model the material a relationship defining the modulus of elasticity and Poisson's ratio as a function of the pavement temperature is needed. Huang et al. (2004) provides such a relationship as defined by the following equations:

$$E(\theta) = 9 \times 10^7 \cdot \theta^{-2.0889} \quad (2)$$

$$\nu(\theta) = 0.0887 \cdot \theta^{0.3791} \quad (3)$$

where  $\theta$ , is the temperature of the pavement in Celsius degrees,  $E$ , the modulus of elasticity (in psi), and  $\nu$ , Poisson's Ratio. As the modulus of elasticity equation approaches infinity as the temperature approaches 0 °C, a maximum value of  $9 \times 10^7$  psi is taken to represent the modulus of elasticity of the pavement at 0 °C. Also, to avoid encountering runtime errors in modeling a minimum value for Poisson's ratio is taken to be  $1 \times 10^{-7}$  at a temperature of 0 °C instead of zero as dictated by the provided equation. Mamlouk et al. (2005) cites several studies concerning the determination of the thermal coefficient of expansion of asphalt

pavements. A value of  $2.63 \times 10^{-5}$  1/K is chosen as it represents a value close to or contained in the ranges of the majority of the studies cited.

The modulus of elasticity of copper is also listed as variable in Table 2 therefore also requiring a relationship with the temperature of the material. Data from [www.engineeringtoolbox.com](http://www.engineeringtoolbox.com) (2009) allows the development of a relationship to capture the very subtle differences in the modulus of elasticity of the copper alloy as a function of temperature given in the following linear regression equation:

$$E(\theta) = -5417 \cdot \theta + 17107360 \quad (4)$$

where  $\theta$ , is the temperature of the copper (in degrees Celsius), and E, the modulus of elasticity (in psi). COMSOL's material library suggests a Poisson's ratio of 0.35 for copper. The two remaining structural material properties, the coefficient of thermal expansion and the yield strength, require the selection of a particular alloy of copper. [Copper.org](http://Copper.org) (2009) lists C12200 as an alloy used in common household piping as well as other heating applications. As listed in Table 2, the thermal coefficient of expansion of this alloy is  $1.71 \times 10^{-5}$  1/K and the yield strength is listed as up to 50,000 psi.

Copper serves as the base pipe material to which other materials are compared, therefore a pipe size needs to be selected based on what is commonly available. Type K possesses the greatest wall thickness of the common household pipes and thus provides the greatest potential to survive loading. A  $\frac{3}{4}$ " nominal diameter is chosen to match the diameter of the pipe used in the field experiments of Section 2.3. In the economic analysis to follow a  $\frac{3}{4}$ " Type K CS12200 Copper pipe is used.

### **3.2. Economic Analysis**

It is necessary for the proposed solution to be economically feasible if applied for purposes other than research. Energy savings considers the total amount of energy harvested from the asphalt pavement. This is compared to an equivalent amount of electricity that would have been consumed from the grid to achieve the same end result. Economic feasibility entails achieving a level of energy savings greater to the cost of the installation and maintenance within a reasonable period of time. This length of time is termed the 'payback period' for that design.

First, a location for the installation of the pipe network must be chosen. Four locations were selected for analysis: Phoenix, Arizona; Houston, Texas; Miami, Florida; and Boston, Massachusetts. Initial assumptions would expect the three locations in the Southern United States to have a reduced payback period due to the higher year-round ambient temperatures. In addition the three locations lie closer to the equator resulting in greater intensity of exposure to solar radiation, the source of the harvested energy. Conversely, Boston, MA would have a longer payback period due to the shifts in temperature with the seasons as well as the increased latitude. Results from the four locations will parallel the climatic behaviors of each of the locations.

An Excel spreadsheet was programmed using the contained Visual Basic software to evaluate the economic performance and provide design options for the proposed solution. Once a location is chosen for evaluation, several items relative to that location must be acquired such the location's latitude, longitude, and time offset from Greenwich Mean Time and entered into the appropriate locations on the spreadsheet. In addition, ambient air temperature readings (in degrees Fahrenheit) for a period of one year must be obtained

from the National Oceanic and Atmospheric Administration (NOAA) or an equivalent source. Dimensions of the pipe as well as the thermal properties of the passing fluid are required. Lastly, the associated costs of the materials and the equipment as well as the expected maintenance costs must be entered. This concludes the 'Input' worksheet of the spreadsheet. An example 'Input' worksheet is located in Appendix A.

The programmed macro proceeds to read and store all of the input. For each of the temperature readings it recognizes the ten character time code (YRMODAHRMN) on the line within the NOAA data file containing the reading, representing the year, month, day, hour, minute. As an example, 200709010000 represents September 1, 2007 00:00. For each day, the maximum and minimum as well as the monthly mean air temperatures are determined and presented as the first set of output on the second page of the spreadsheet titled 'Statistics'. All output temperatures and inputs into the subsequent calculations are in degrees Celsius.

Viljoen (2001) provides a method for the determination of the temperature profile within asphalt pavements as a function of the ambient air temperature and other environmental characteristics of an installation location. The maximum asphalt surface temperature,  $T_{s(max)}$ , for each day is determined according to the following equation (Denneman, 2007):

$$T_{s(max)} = T_{air(max)} + 24.5(\cos Z_n)^2 \times C \quad (5)$$

where  $T_{air(max)}$  represents the maximum ambient air temperature,  $Z_n$  represents the zenith angle at solar noon calculated using the General Solar Position Calculations equations provided by NOAA (NOAA, 2009). This term accounts for the influence of solar exposure on the surface temperature of the asphalt pavement. The zenith angle at solar noon is a

function of the latitude of the location resulting in higher values for locations closer to the equator.  $C$ , an empirical coefficient, termed the ‘cloud cover index’, accounts for the presence of clouds in the sky reducing exposure level to solar radiation. On days where the maximum temperature is greater than 30° C, this value is taken to be 1.1; for day where the temperature is less than 30° C but greater than the monthly mean temperature this value is taken to be 1.0; otherwise, this value is taken to be 0.25.

Determining the minimum asphalt surface temperature,  $T_{s(min)}$ , requires only the minimum air temperature,  $T_{air(min)}$ , as follows (Denneman, 2007):

$$T_{s(min)} = 0.89T_{air(min)} + 5.2 \quad (6)$$

The maximum and minimum asphalt surface temperatures for each day are the last of the output provided on the ‘Statistics’ worksheet. An example ‘Statistics’ worksheet is located in Appendix A.

The equations provided by Viljoen (2001) also allow calculation of the asphalt temperatures at a depth,  $d$  (in millimeters). The maximum asphalt temperature at depth,  $T_{d(max)}$ , and minimum asphalt temperature,  $T_{d(min)}$ , are determined according to the following equations (Denneman, 2007):

$$T_{d(max)} = T_{s(max)}(1 - 4.237 \times 10^{-3}d + 2.95 \times 10^{-5}d^2 - 8.53 \times 10^{-8}d^3) \quad (7)$$

$$T_{d(min)} = T_{s(min)} + 3.7 \times 10^{-2}d - 6.29 \times 10^{-5}d^2 \quad (8)$$

requiring the maximum,  $T_{s(max)}$ , and minimum  $T_{s(min)}$ , asphalt surface temperatures respectively. Equations (5), (6), (7), and (8) are completed for each day of the year and stored in a matrix providing input for the next series of hourly calculations.

The next phase of calculations involves developing the hourly temperature profiles at the varying depths with in the pavement. By default, the spreadsheet calculates the

profile at the depths of 0, 25, 50, 75, 100, 125, and 150 millimeters corresponding to approximately 0, 1, 2, 3, 4, 5, and 6 inches below the surface. It is necessary to introduce a parameter,  $\alpha$ , which addresses the time lag (in hours) in the temperature response of the pavement through its depth,  $d$  (in millimeters) associated with its low thermal conductivity (Denneman, 2007):

$$\alpha = 2 + \frac{d}{50} \quad (9)$$

An additional time parameter,  $\beta$  (in hours), accounts for high thermal capacity of the asphalt pavement. This value, taken as 1.5 hours is realized through the pavement reaching its minimum temperature after sunrise.

The daily temperature profile consists of a heating and a cooling phase. The heating phase, which begins at a time of day equal to that of sunrise,  $t_r$ , plus  $\beta$  is governed by the following sinusoidal equation (Denneman, 2007):

$$T_{d(t)} = T_{d(min)} + [T_{d(max)} - T_{d(min)}] \sin \left[ \pi \frac{(t-t_r-\beta)}{DL+2(\alpha-\beta)} \right] \quad (10)$$

where  $T_{d(t)}$  is the temperature at depth at a time of day  $t$ , in hours, given as a function of the maximum and minimum temperatures at that depth,  $T_{d(max)}$  and  $T_{d(min)}$ , as well as the time of sunrise,  $t_r$ , and the length of day  $DL$ , in hours as calculated according to the General Solar Position Calculations provided by NOAA.

Sunset begins the cooling phase of the temperature where the following equation applies (Denneman, 2007):

$$T_{d(t)} = T_{d(min)}^n + [T_{d(t_s)} - T_{d(min)}^n] \exp \left[ -\frac{\gamma(t-t_s)}{24-DL+\beta} \right] \quad (11)$$

In this equation,  $T_{d(t)}$  still represents the temperature at depth at a time of day  $t$ , in hours, and  $DL$ , the length of day in hours, however, the  $T_{d(t_s)}$  represents temperature of the

pavement at time of sunset  $t_s$  in hours, and  $T_{d(min)}$ , the minimum temperature of the pavement at depth of the next day. The cooling phase realizes an exponential decay from the temperature at depth of the pavement at sunset to the minimum temperature at the depth the next morning. In doing so, the profile maintains continuity from day to day. Figure 10 presents an example 24-hour period of the temperature profile containing the maximum asphalt temperature of the year for Houston, TX. During each phase the temperature profiles cross whereby by the end of the cooling phase the temperature at depth is greater than that of the surface. This crossover recognizes the slow travel of heat through the depth of the pavement consistent with its low thermal conductivity as well as its high thermal capacity whereby the lower layers of the pavement are capable of supplying heat to the upper layers of the pavement well after the cooling phase has begun.

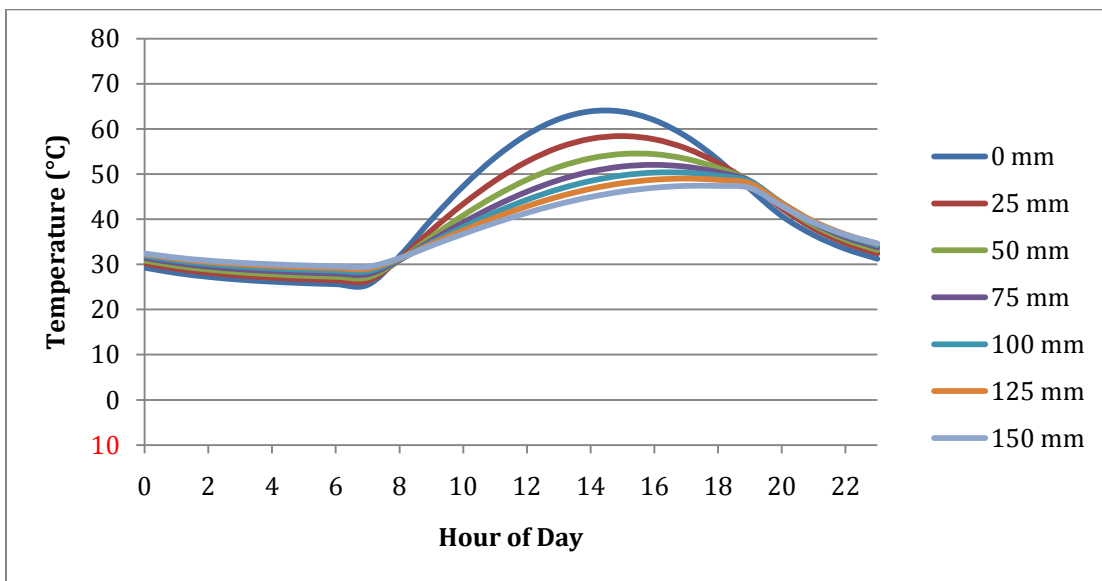


Figure 10: Temperature profile for 24-hour period containing the maximum pavement temperature (Houston, TX) (0, 1, 2, 3, 4, 5, 6 inch pavement depths)

The spreadsheet determines and stores the temperature at each of the depths for every hour of the year and presents the values in a separate worksheet titled 'Profile'. On the fourth worksheet, titled 'Profile Summary', the spreadsheet displays a chart of the

asphalt temperature profile of the surface and a depth of 150 mm for the entire year. This chart provides visual representation of the economic feasibility and mimics the climatic behavior of the location. The day at which the maximum and minimum temperatures occur within the pavement are selected for closer investigation. The temperature profiles for all depths of the 24-hour period in which the maximum and minimum temperatures occur are then presented in chart format to verify the behavior of the equations. An example of the 'Profile' and the 'Profile Summary' worksheets are presented in Appendix A.

The temperature profiles provide a method to quantitatively measure the amount of heat energy that can be extracted from the asphalt pavements. Higher asphalt pavement temperatures result in a greater energy savings while lower temperatures result in a reduced energy savings. The variations in the temperature profile affect the overall performance as well where consistently high temperatures are more favorable than seasonal variations.

For a given location the available inlet water temperature can be determined by a simple measurement with thermometer and may vary with both location and season. Conservatively, this temperature can be assumed as 20° C. This water enters the pipe network at the known (or assumed) temperature and exits the pipe network at a temperature equal to that of the pavement at the given depth of pipe placement. For every hour of the year the amount of energy harvested,  $H$ , of the pavement can be determined from the difference of the outlet and inlet water temperatures,  $\Delta T_{water}$ , according to the following equation:

$$H = m_{water}c_{water}\Delta T_{water} \quad (12)$$

where  $c_{water}$  refers to the specific heat capacity of the water and  $m_{water}$ , the total mass passed in that hour. The mass of water passed through the pipe network is related to the chosen flow rate of the water as follows:

$$m_{water} = Q\rho_{water} \quad (13)$$

where,  $Q$  represents the flow rate of water, and  $\rho_{water}$ , the density of water taking care to keep consistent units. Summing each hour interval over the entire year results in a total amount of energy harvested. Multiplying the total amount of energy harvested by the current price for electricity yields the energy savings for that location.

The spreadsheet calculates the energy savings for flow rates including 1 to 30 liters per minute. The fluid flow rate influences the length of the pipe network whereby higher flow rates requires a greater length of pipe for the fluid to achieve the same temperature as the surrounding pavement. Heat flows from the pavement through the wall of the pipe through conduction and then to the fluid through convection. The pipe length is calculated according to the following derived equation:

$$L = \frac{\dot{m}c_{water}}{3.66\pi k_{water}} \ln\left(\frac{T_{d(max)} - (T_{d(max)} - T_{dev})}{T_{d(max)} - T_{inlet}}\right) \quad (14)$$

where  $m$ , represents the mass flow rate of the passing water,  $c_{water}$ , the specific heat capacity of the water,  $k_{water}$ , the thermal conductivity of water,  $T_{d(max)}$ , the maximum temperature of the pavement at depth experienced during the year,  $T_{dev}$ , a variable chosen by the user to design for an outlet temperature lower than the maximum temperature, and  $T_{inlet}$ , the measured inlet water temperature for practical considerations. Equation 14 relies on the assumption that pipe walls remain at a constant temperature equal to that of the surrounding pavement. This assumption is valid because of the high thermal capacity of asphalt pavement; however, the flowing water will serve to reduce the temperature of the

pavement over time to lower temperatures than predicted by the spreadsheet. As such, the energy savings obtained from harvesting the thermal may be overestimated.

Initial capital costs consist of all of the material costs, such as copper piping, and equipment costs, such as the cost of the pump and monitoring systems. The cost of the pipe network varies with its length. There is a material cost associated with the installation of the pipe network as well as an operational cost. The operational cost consists of the grid power required to pump the fluid through the pipe network. A longer pipe network requires more power due to the presence of friction between the fluid and the walls of the pipe. For each flow rate and depth of pipe, the spreadsheet calculates the power required to pump the fluid as well as the yearly energy cost. The total yearly cost is this yearly energy cost plus any additional expected maintenance costs for the year. The net yearly savings is the subtraction to the total yearly cost from the previously calculated total energy savings. The payback period for a particular design, or depth and flow rate combination, is thus determined by dividing the total initial capital cost by the net yearly savings.

The spreadsheet outputs a formatted sheet for each depth of pipe. Contained on the sheet is a summary of the input values for properties of the fluid and pipe as well as the costs. For each design, organized sequentially by flow rate, the length of the pipe network, the required pump power, yearly energy consumed from the grid, energy harnessed from the pavement, initial capital cost, net yearly savings, and payback period are reported. This information reported on the 'Results' worksheet, provides a concise summary of potential designs for a client to make an informed decision. The results of all the intermediate calculations for reference if needed are contained within the 'RAW' worksheet. Retaining

this spreadsheet provides the end user with an effective way to verify that each calculation is correct by the end user. An example of the 'Results' and 'RAW' worksheets can be found in Appendix A. The presentation of all output marks the termination of the programmed macro. A design can then be selected from the results presented for further investigation through computer modeling.

### 3.3. Computer Modeling

If the previous spreadsheet determines that an installation location is economically feasible, the next step may be taken to determine if the pipe network will survive structurally under loading. This can be achieved most effectively through the implementation of COMSOL Multiphysics© a finite element software that allows the study of thermal and mechanical effects simultaneously. The model geometry can be created as shown in Figure 11 to represent a slab that is 36 inches long, 36 inches wide, and 12 inches deep with a  $\frac{3}{4}$  inch nominal diameter pipe centered at a variable depth of 1 to 6 inches from the surface of the slab. Preliminary analysis shows that this width of slab is great enough to avoid interference from the boundary conditions.

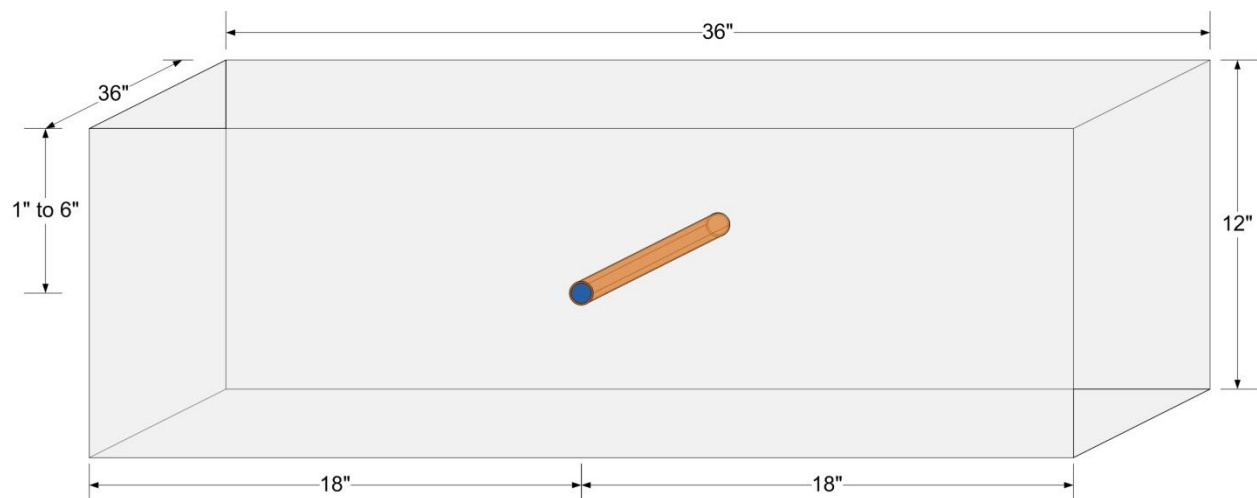


Figure 11: COMSOL model dimensions (length into page)

The software automatically divides the geometry into different subdomains to which material properties must be attached. The three subdomains consist of the hot mix asphalt (HMA), the pipe, and the flowing water. Appropriate material properties from Section 3.1 must be specified for each subdomain. The software also automatically detects internal and external boundaries. All internal boundaries setting are ignored as only continuity needs to be maintained. External boundary conditions representative of field conditions must be specified as follows:

- Base and side faces along the length
  - Thermal: Insulation/Symmetry
  - Structural: Fixed
- Sides perpendicular to pipe
  - Thermal: Insulation/Symmetry
  - Structural: Free
- Pipe inlet
  - Thermal: Fixed temperature (293 K)
  - Structural: Free
- Pipe outlet
  - Thermal: Convective flux
  - Structural: Free
- Surface
  - Thermal: Heat flux
    - Inward heat flux:  $1000 \text{ W/m}^2$
    - Heat transfer coefficient:  $4.64 \text{ W}/(\text{m}^2\cdot\text{K})$
    - External temperature: 293 K
    - Radiation type: Surface-to-ambient
    - Emissivity: 0.9
    - Ambient temperature: 293K
  - Structural: Free
    - 6" radius circle centered
    - 90 psi distributed load

The thermal boundary conditions establish the different paths which energy may enter and leave the slab. The inward heat flux serves as the solar radiation source with an amount being reflected back to the atmosphere dictated by the emissivity and the ambient air temperature. This value for inward heat flux is conservative as Figure 5 indicates a

greater solar exposure at the testing location of Worcester, Massachusetts. The presence of the heat transfer coefficient allows heat energy to escape from the surface due to convection. A fixed temperature condition at the pipe inlet ensures that a flow of water is provided at 20 degrees Celsius. The convective flux at the outlet allows the heated water to exit the system taking with it the energy harnessed from the pavement surrounding the pipe.

The structural boundary conditions represent the loading conditions expected in the field. If an installation is to be placed in a road or a parking lot it can expect to undergo loading from many different vehicles over the course of its existence. To represent a typical truck tire load, a 90 psi distributed load is placed at the center of the slab. The dimensions of the slab are great enough so that the fixed boundary conditions do not influence the stresses developed in the pavement.

The coupling of the heat transfer and structural mechanic modules of COMSOL allows the investigation of the structural behavior of different pipe materials and pipe depths over a variety of temperature. The heat transfer module provides a means to change the temperature of the materials to discrete values as well as to change the temperature through modeling the complete proposed solution. A change in the temperature of the materials results in a change in their structural behavior especially in the case of HMA as described in Section 3.1. Discrete temperature analysis provides a method to directly compare the results of specific changes to the model such as the pipe material or the depth of pipe.

## **4. Results**

Background research and initial field experiments established the conceptual feasibility of the proposed solution. Spreadsheet will establish the economic feasibility of the proposed solution in certain locations. Design taken, from its output can then be modeled in finite element software to determine the structural survivability of the proposed solution.

### **4.1. Economic Analysis**

The economic feasibility of four locations were investigated using the programmed spreadsheet. Three of these locations, Phoenix, AZ, Houston, TX, and Miami, FL are in the Southern United States and were presumed to be feasible locations for the installation of a pipe network within an asphalt pavement. An additional location in the Northern United States, Boston, MA was chosen for investigation to verify the behavior of the spreadsheet through contrast. The appropriate parameters for each location were entered into the spreadsheet including the associated air temperature data. The programmed macro was then initiated and designs for each of the locations were generated. Figure 12 contains the yearly temperature profiles for each of the four locations under investigation.

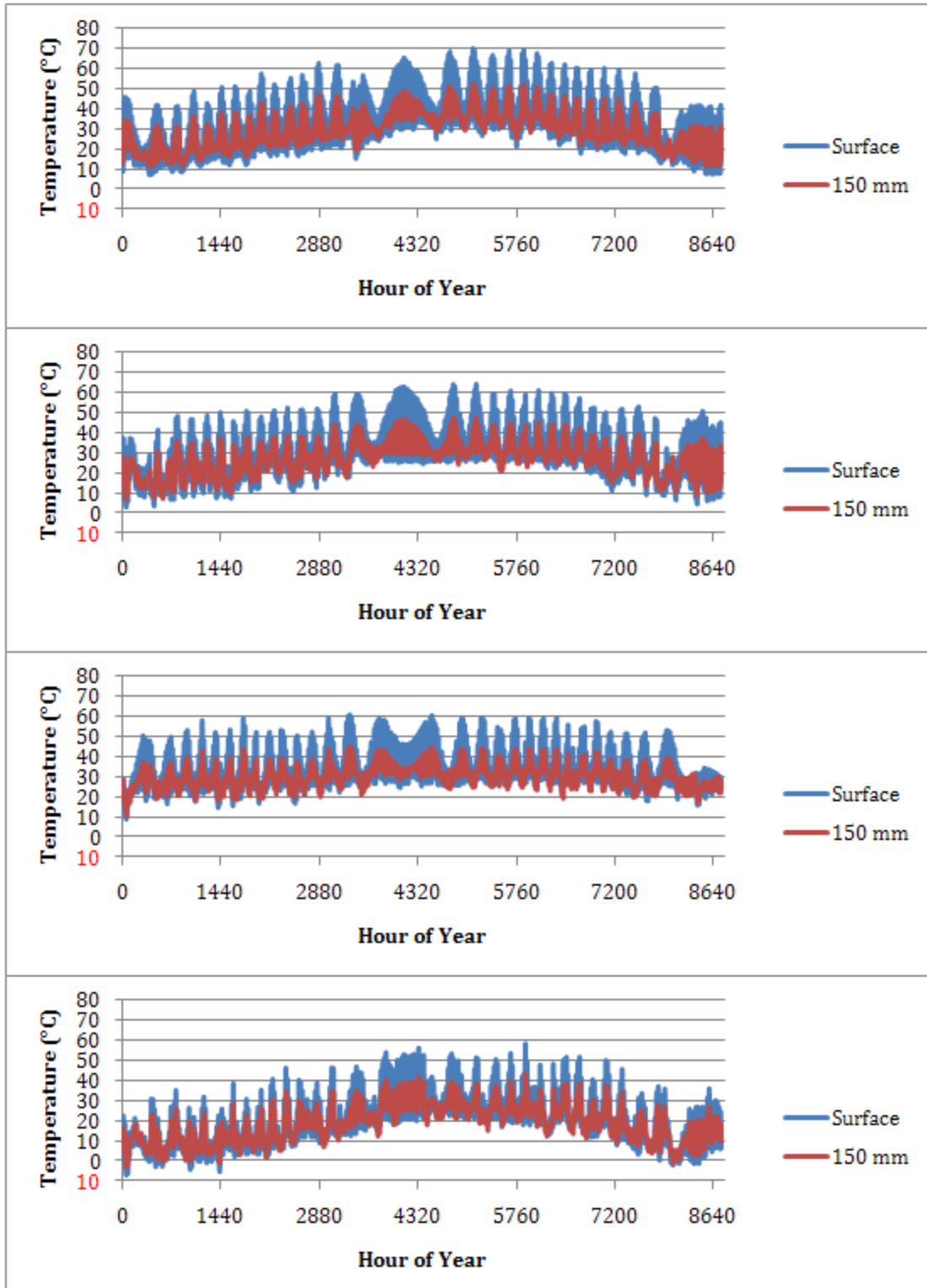


Figure 12: One-year pavement temperature profiles: (1) Phoenix, AZ (2) Houston, TX (3) Miami, FL (4) Boston, MA

Each of the four temperature profiles exhibit different behaviors. Phoenix, AZ experiences the highest pavement temperature of the four locations reaching 70 °C for a significant portion of the summer months. This results in an increased yield of energy from the asphalt during this period of time. This magnitude parallels the extremely high temperatures experienced by that region of the United States during the summer months. The temperatures then trail off sharply as the winter months approach. Houston, TX also witnesses seasonal changes in temperature; however, the shift from one season to the next is more gradual providing a similar number of days where the asphalt temperature is above 20 °C but at a lower maximum temperature. It is critical that the temperature of the asphalt be greater than 20 °C as this is the assumed (or a different value if measured) of the water entering the pipe network. Thus, the system is assumed to be running and extracting thermal energy from the pavement whenever the temperature of the pavement is greater than this value. If the system were to run when the temperature of the pavement were less than that of the inlet water then energy would be lost in pumping the fluid through the pipe network. In energy calculations, this situation is omitted as it is assumed that the system would be stopped.

Miami, FL, while attaining the lowest maximum pavement temperature of the three southern locations, has pavement temperatures above 20 °C for nearly all of the days of the year. This allows the system to be running continuously throughout the year to harvest the thermal energy from the pavement. Boston, MA peaks at the lowest temperature of the four locations and remains over 20 °C consistently for the least amount of time resulting in a very small window during which the system would be active. This was expected as Boston, MA is located the furthest away from the equator resulting in reduced solar

exposure as well as drastic changes in climate from the changing seasons. In some cases the pavement temperature drops below freezing in which case it would be impossible for the system to function if the fluid of choice is water.

In summary, the temperature profiles shown in Figure 12 mimic the climatic conditions of each of the locations validating the equations used to determine the temperature profiles. The contrast in the temperature profiles demonstrates the sensitivity of the calculation to the climate of the location. This accuracy and sensitivity support the use of the temperature profile in accurately determining the amount of energy available for capture and developing pipe network designs to be used in computer modeling.

Table 3 presents a summary of the amount of energy harvested and corresponding payback period for an installation of a pipe network at each of the four locations. For appropriate comparison, the same design was chosen for each location: a fluid flow rate of 13 liters per minute and a depth of pipe of 50 millimeters.

Table 3: Economic analysis summary

<b>Location</b>	<b>Latitude</b>	<b>Network Length (m)</b>	<b>Energy Harnessed (kWh)</b>	<b>Payback Period (years)</b>
<b>Phoenix, AZ</b>	33.43	479	79567	3.7
<b>Houston, TX</b>	29.97	460	64756	4.8
<b>Miami, FL</b>	25.82	449	84547	3.4
<b>Boston, MA</b>	42.37	439	25592	27.0

Miami, FL has the shortest payback period due to the number of days over 20 °C but requires the shortest pipe network of the three southern location which is consistent with having the lowest maximum temperature pavement temperature at depth of the three locations. Phoenix achieves the second lowest payback period but requires the longest pipe network as it possesses the highest maximum pavement temperature at depth.

Houston, TX witnesses a good payback period due to the increased number of days over 20

°C as compared Phoenix, but at a lower maximum pavement temperature at depth than Phoenix. Houston, however, has far fewer days over 20 °C as compared to Miami, FL which almost account for the increased payback period. Lastly, Boston, MA has the least favorable payback period and shortest pipe network because it possesses the lowest maximum pavement temperature at depth as well as very few days over 20 °C as compared to the three southern locations. The results presented are consistent with the behaviors of the temperature profiles of each of the locations.

#### 4.2. Computer Modeling

With the economic feasibility of the proposed solution established by the programmed spreadsheet, computer modeling of the proposed solution to investigate the structural survivability was completed using COMSOL Multiphysics© finite element software. The software provides both numerical and graphical output. Figure 13 is an example of the thermal graphical output illustrating the temperature profile in the pavement due to solar exposure both before the flow of water and well after the flow of water. Deep red indicates the highest temperature in the pavement at the time while deep blue indicates the lowest temperature.

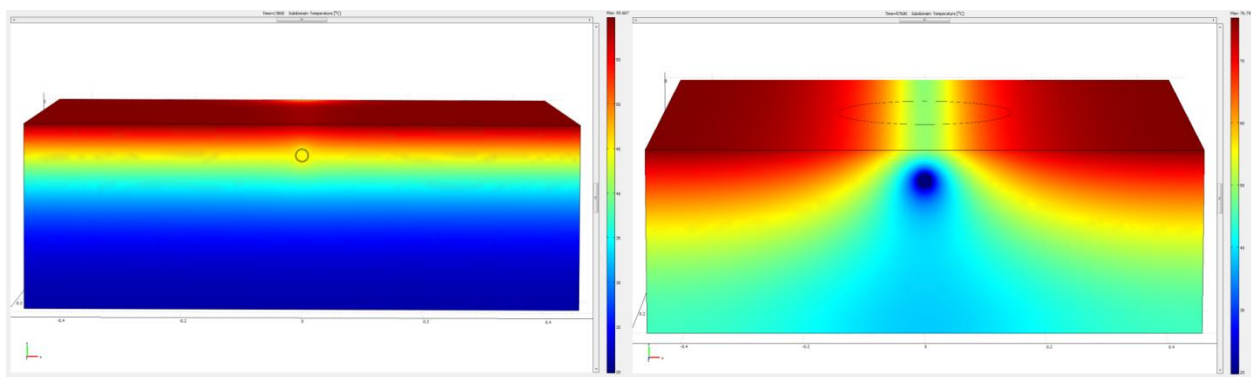


Figure 13: Example thermal solution (left) before water flow, (right) after flow

Similar graphical output can be obtained for the stresses in the pavement due to loading as shown in Figure 14. For the figure on the left the plot range has been adjusted to highlight the contrast in stresses in the pipe. As with the temperature plots, red indicates the greatest magnitude of Von Mises stress and blue the lowest magnitude. The surrounding pavement appears as one color due to extreme difference in magnitudes of stresses realized by the pipe and the pavement. Adjusting the plot range to the magnitude of stresses realized only in the pavement highlights the contrast in stresses in the pavement as shown in the right part of Figure 14.

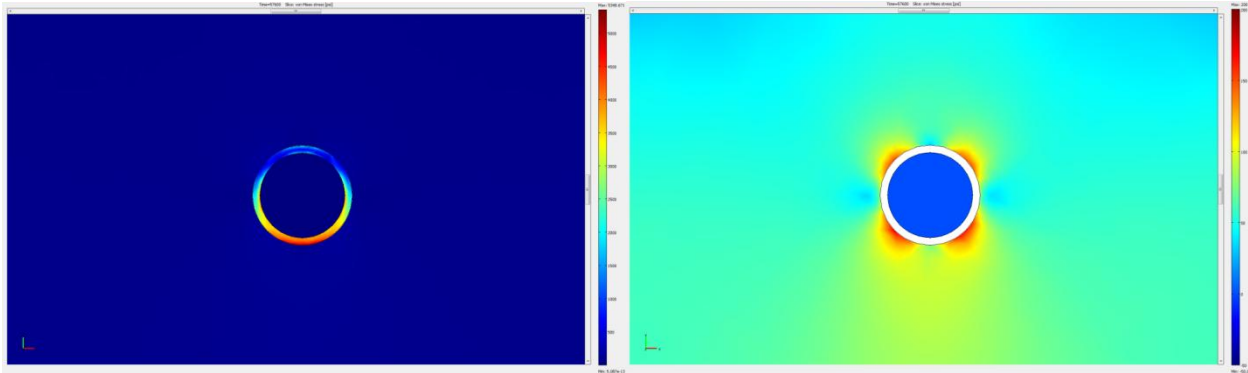


Figure 14: Example structural solution (left) pipe stresses, (right) pavement stresses

Studies of this graphical output for several depths of pipe resulted in the identification of 11 possible points at which the critical stress in the pipe and in the pavement might occur. Figure 15 illustrates the 11 points on a diagram of the pipe. Six locations in the pipe include in the inner and outer walls of the top, side, and base of the pipe. Locations in the pavement begin just outside the top of the pipe and occur at 45-degree intervals, tracing around the circumference of the pipe to its base.

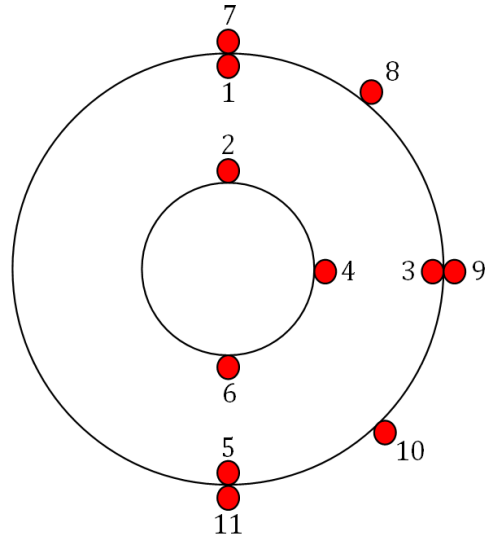


Figure 15: Points of investigation for critical stresses

Preliminary studies of the numerical values of the stresses indicate that the critical or maximum stress in the pipe occurs at point 5, the outer wall at the base of the pipe. Similar studies indicate the maximum stress in the pavement occurs at point 9, just outside the right wall of the pipe. This determination established a basis for comparison for the studies to follow. Three studies were conducted with the critical stress obtained from points 5 and 9.

#### 4.2.1. Study One: Constant vs. Varying Poisson's Ratio

A study was conducted to determine the sensitivity of the stress in the pipe and in the pavement to the Poisson's ratio for the hot mix asphalt (HMA). A discrete temperature analysis was performed incrementing the temperature of the materials from 0 degrees Celsius to 70 degrees Celsius in increments of 10 Celsius degrees. In the first model a constant value of 0.35 was used for Poisson's ratio of the HMA. In the second model, a varying value for Poisson's ratio according to Equation 3 of Section 3.1 was used. Copper was chosen as the pipe material for both models. The maximum stresses for a pipe depth

of 2 inches in the pipe and pavement obtained from points 5 and 9 for the entire temperature range are plotted in Figure 16. The results show no significant difference in the level of stresses using a varying Poisson's ratio over a constant value of 0.35. At temperatures above 40 degrees Celsius a varying Poisson's ratio predicts slightly higher stresses in the pipe than using a constant value. In contrast, a varying Poisson's ratio predicts higher stresses in the pavement than a constant value. The stresses in the copper pipe are greater at higher temperatures reaching approximately 13000 psi but well under the yield strength of the material of 50000 psi. The stresses in the pavement are greater at a lower temperature, reaching a value of 210 psi which is much closer to the yield strength of 300 psi. Similar results were found at pipe depths of four and six inches shown in Figure 25 and Figure 26 located in Appendix B. As such, the stresses in the pavement are the limiting stresses. Continued use of the temperature-varying value for Poisson's ratio of HMA builds in additional conservatism into the determination of pavement stresses in other studies.

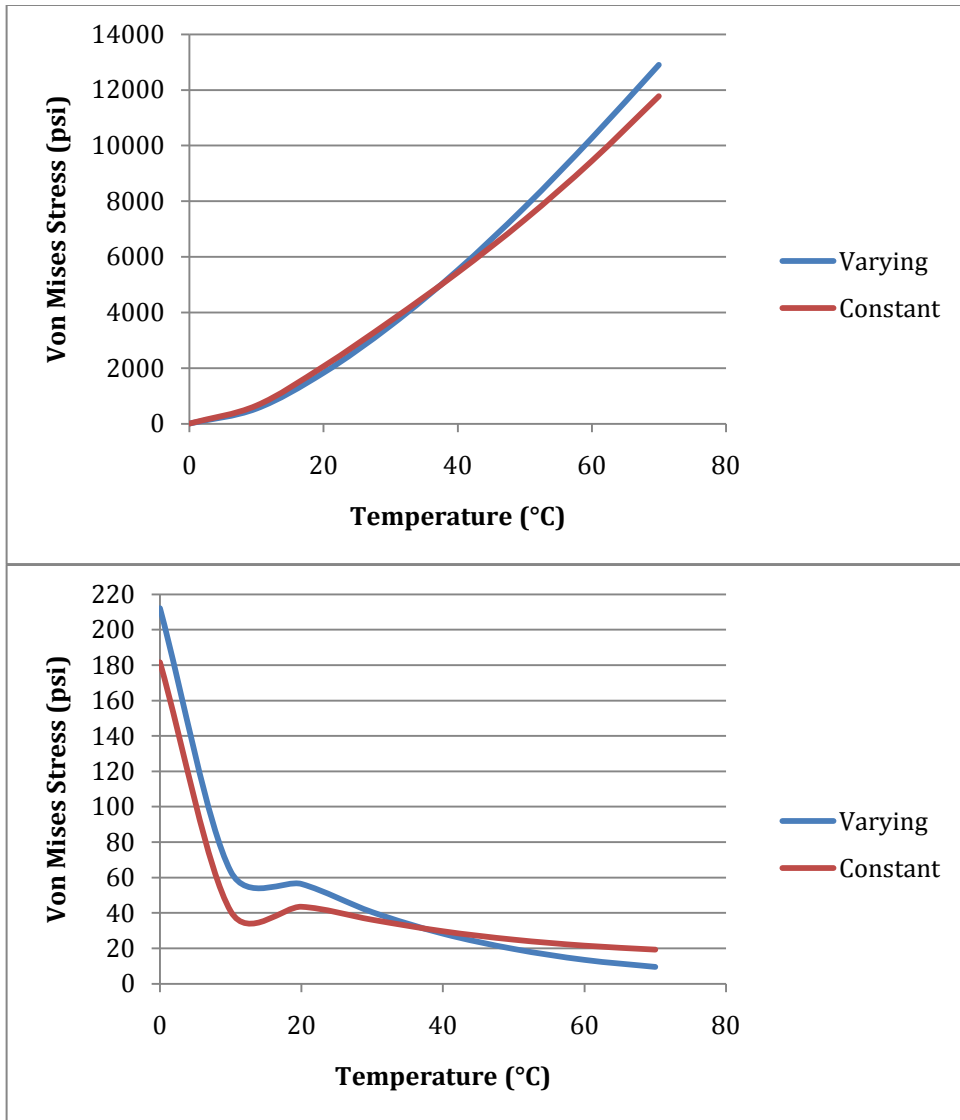


Figure 16: Constant vs. varying Poisson's Ratio (2" pipe depth) (top) copper pipe (bottom) HMA

**4.2.2. Study Two: Stress vs. Pipe Depth**

A second study was conducted to investigate the stresses in the pipe and pavements as a function of the depth of the pipe. Similar to Section 4.2.1, the temperature of the materials was varied in increments of 10 Celsius degrees from 0 degrees Celsius to 70 degrees Celsius to represent the range of temperature an installation might witness. In this analysis, the primary variable was the depth of the copper pipe as the temperature-varying value for Poisson's ratio of HMA was utilized. Pipe depths of 1, 2, 3, 4, 5, and 6 inches were

modeled, and the critical stresses obtained from points 5 and 9 for each depth. Figure 17 plots the maximum pipe and pavement stresses as a function of the depth of the pipe. The greatest stress in the pavement occurs at the most shallow depth of 1 inch while the greatest stress in the pipe occurred at a middle depth of 2 and 3 inches. Past a depth 4 inches, stresses in the pipe and the pavement both begin to reduce. At all depths, the stresses within the pipe and the pavement are below that of the yield strengths of the materials, which argues for the survival of the pipe network for the depths modeled.

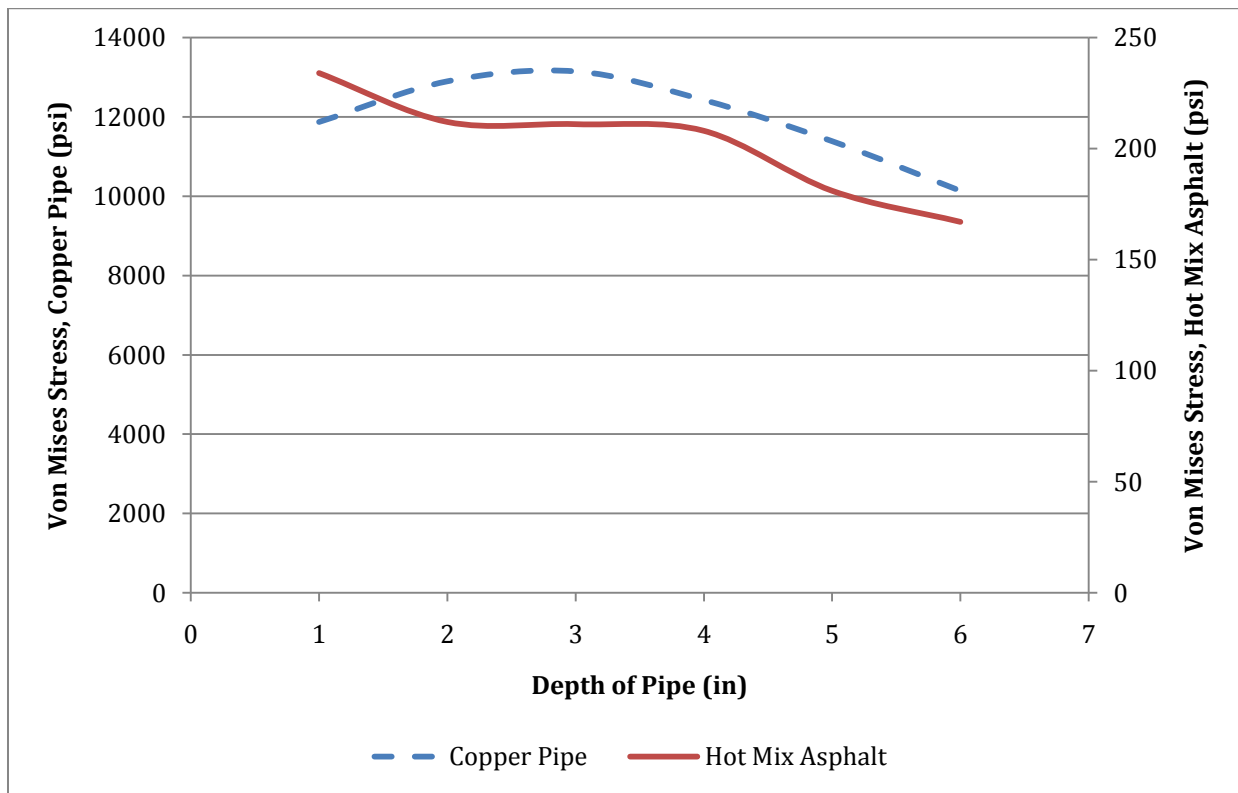


Figure 17: Stress vs. pipe depth

#### 4.2.3. Study Three: Stress vs. Temperature for Different Pipe Materials

A third study was conducted to determine the behavior of the proposed solution using alternative pipe materials. In this study two other materials, PVC and PEX (cross-linked polyethylene flexible piping), were investigated in place of the copper pipe. These materials were subjected to the same temperature sweep as copper, exploring

temperatures of 0 to 70 degree Celsius in 10 Celsius degree increments. The thickness of the pipe wall was not changed in order to directly compare the effects of different material properties. Figure 18 presents the results of this study, plotting the stresses in the pipe and the pavement as a function of temperature with a separate line representing each material. Numerical values are summarized in Table 4.

Copper realizes the greatest stress of the three pipe materials due to its high modulus of elasticity. As the temperature of asphalt increases, its stiffness decreases significantly causing the stiffer pipe to carry more of the load. This is confirmed by an increase in the stress within the pipe material coupled by a decrease in stress within the pavement. Similar behavior is exhibited by each of the materials modeled but to a lesser extent. PEX, which has the lowest modulus of elasticity, witnesses the least amount of stress. As such, it also results in the greatest magnitude of stresses in the pavement even at increased temperature. The closer proximity of moduli of elasticity requires the pavement to carry a greater portion of the load as compared to the stiffer copper. PVC has a similar relationship with stress values in the pipe and pavement lying between that of copper and PEX. All three materials, however realize stress that are within their yield strength supporting the survival of the pipe network utilizing these materials.

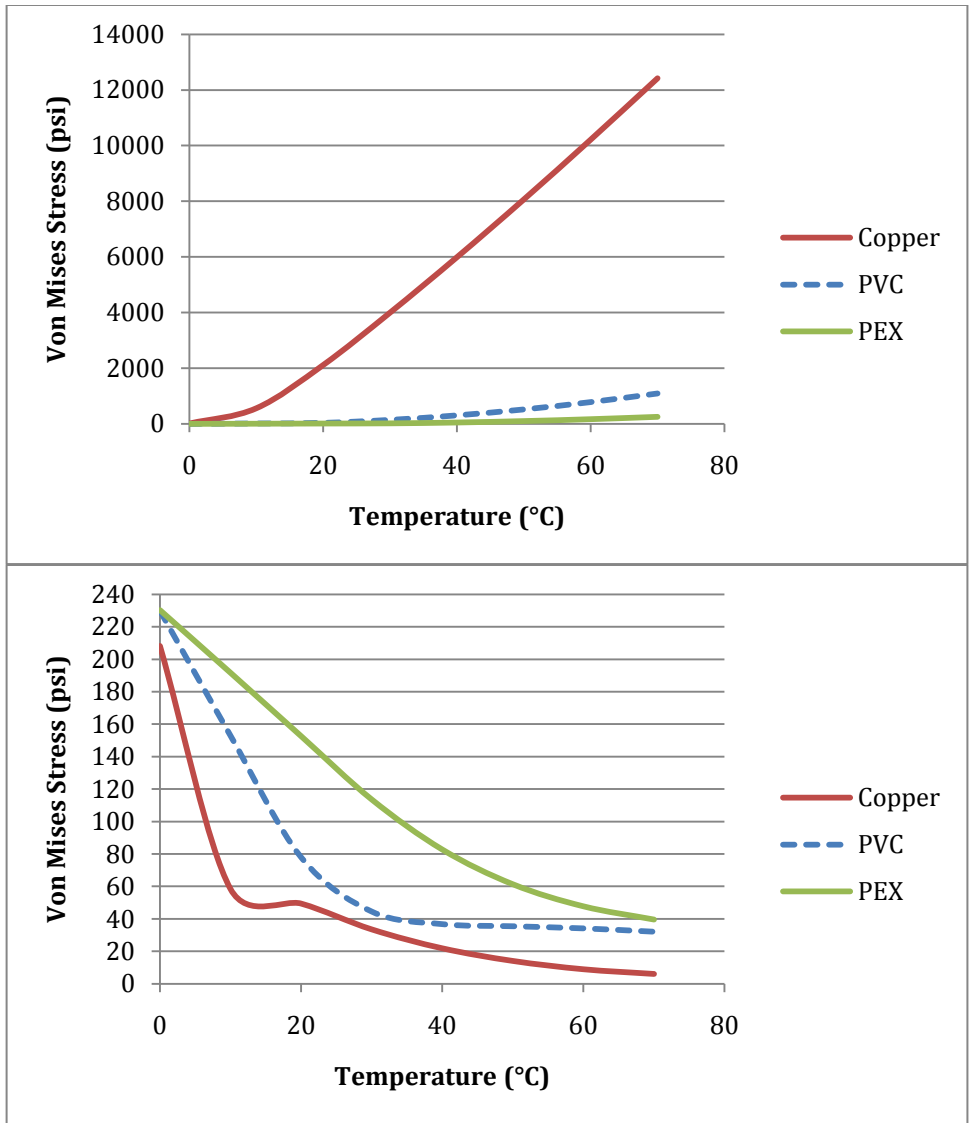


Figure 18: Stress vs. temperature for copper, PVC, and PEX (4" pipe depth)

Table 4: Stress summary

<b>Material</b>	<b>Tensile Yield Strength (psi)</b>	<b>Maximum Stress (psi)</b>	
		<b>Pipe</b>	<b>Pavement (HMA)</b>
<b>Copper</b>	50000	12426	208
<b>PVC</b>	7450	1084	230
<b>PEX</b>	2180	244	230
<b>HMA</b>	300	-	-

## 5. Conclusions and Recommendations

A proposed solution has been developed to harness the thermal energy from asphalt pavements to reduce the urban heat island effect. A fluid flowing through a pipe network in the pavement extracts the thermal energy from the pavement which heats the fluid. A long enough pipe network raises the temperature of the water to that of the pavement at depth. The heated water provides an economic advantage through its utility: it may be used in power generation, stored for later use, or simply used as hot water which now requires much less energy to heat to desired temperatures.

A spreadsheet was programmed to determine the economic feasibility of the proposed solution for four locations: Phoenix, AZ; Houston, TX; Miami, FL; and Boston, MA. In future studies, other locations may be chosen as the spreadsheet allows the study of any location for which there is air temperature data available. It was determined that the proposed solution was economically feasible at the three southern locations but not in Boston, MA. There may be a fluid flow rate, in Boston, MA, that is sufficiently high enough to achieve a similar payback period to those in the Southern United States, however an estimate for such a high flow rate using the spreadsheet may be incorrect. The spreadsheet does not take into account the reduction in the pavement temperature as a result of the passing fluid. It assumes that no matter the flow rate, the asphalt remains at the same temperature at that depth. As such the spreadsheet will produce an upper-bound solution and reports a more favorable payback than can be achieved. It was also recognized that the depth of the pipe only minimally affects the payback period of the system.

Additional studies through computer modeling could be conducted to investigate the change in temperature of the pavement as a function of the flow rate of the fluid. A range of flow rates could be investigated, and another module added to the spreadsheet code to adjust the available energy accordingly.

Three studies were conducted using the finite element software COMSOL Multiphysics© which allowed the simultaneous evaluation of the thermal and structural behavior of the proposed solution. The first study established the use of a temperature-varying value to be used for Poisson's ratio as it provided an additional level of conservatism in determination of pavement stresses. The second study of temperature versus depth presented a maximum stress in the pavement for a pipe depth less than two inches. It is likely that a pipe would not be placed at this depth as there would only be minimal cover for the pipe supporting the presence of surface cracks. A minimal depth of pipe recommended by the Copper Development Association (2006) for copper pipes is 1 ½" inches. Since the depth of the pipe has a minimal effect on the payback period, the pipe should be placed at a depth of 4 inches or greater, the depth at which the stresses begin to decrease appreciably with depth for both the pipe and the pavement.

The third study, looking at different pipe materials as a replacement for copper, evaluated structural survivability. In all, three materials (copper, PVC, and PEX) were investigated. The stresses in the pipe and the pavement were below the yield strengths of the respective materials. While this suggests survivability under a single wheel loading, it does not guarantee any life cycle performance. While the stresses may be low enough to not cause immediate damage to the pipe or the pavement, repeated loading could result in fatigue failure within any of the materials. Additional studies could be conducted to

investigate the effects of repeated loading of a truck tire on the pipe network to determine its length of service. Similar parameter sweeps of temperature and pipe depth could be performed, and a module incorporated into the spreadsheet that reports the expected service life of the system and compares it to the payback period of the system to quickly determine both economic and structural survivability.

Last, further investigation into thermal stresses should be completed. The results presented in this thesis only incorporate stresses from thermal expansion during the heating phase of the asphalt pavement up to the start of the flow of water. Initial studies into this topic suggest that the thermal stresses induced by the sharp change in pipe/pavement temperature due to the introduction of a fluid at a much lower temperature are greater in magnitude than the mechanical stresses that result from the application of the truck tire load. Further studies are needed to support this theory and to determine if survivability is maintained during the cooling period as well.

It has been determined through field experiments that the proposed solution is conceptually feasible. Initial finite element modeling conducted by Chen showed that the proposed solution can be reliably modeled using the COMSOL Multiphysics© software. Spreadsheet analysis of four installation locations proved economic feasibility for the three southern locations. Further computer modeling established the survivability of the proposed situation for the materials studied. The installation of a pipe network in asphalt pavements is economically feasible and will survive the expected loading. The proposed solution serves to reduce the temperature of the pavement, thereby achieving the goal of reducing the urban heat island effect while providing the economic advantages of heated

water, reduced energy consumption for the surrounding structures, and longer pavement life.

## References

- Bondt, A.H., Jansen, R. *Generation and Saving of Energy via Asphalt Pavement Surfaces*. Ooms Nederland Holdingbv. Netherlands. November 2006. <http://www.ooms.nl>
- Chen, B. *Capture Solar Energy and Reduce Heat-Island Effect from Asphalt Pavement*. M.S. Thesis: Worcester Polytechnic Institute (WPI). December 14, 2008
- COMSOL Multiphysics©. *User's Guide*. Version 3.5a. 2008.
- Copper.org. Resources: Standards & Properties – Properties of Wrought and Cast Copper Alloys (C12200). Retrieved on October 2, 2009 from <http://www.copper.org/resources/properties/db/>
- Copper.org. Standards & Properties: Mechanical Properties of Copper and Copper Alloys. Retrieved on November 11, 2009 from [http://www.copper.org/resources/properties/144\\_8/144\\_8.html](http://www.copper.org/resources/properties/144_8/144_8.html)
- Copper Development Association Inc. *The Copper Tube Handbook*. New York, New York. 2006.
- Denneman, E. *The Application of Locally Developed Pavement Temperature Prediction Algorithms in Performance Grade (PG) Binder Selection*. Proceedings of the 26<sup>th</sup> South African Transportation Congress. South Africa: Pretoria. July 2007. Pages: 257-266
- Engineering Toolbox. Young Modulus of Elasticity for Metals and Alloys. Retrieved on November 5, 2009 from [http://www.engineeringtoolbox.com/young-modulus-d\\_773.html](http://www.engineeringtoolbox.com/young-modulus-d_773.html)
- Harvel. PVC Pipe: Superior Quality Piping for a Wide Range of Applications. Retrieved on November 20, 2009 from <http://www.harvel.com/piping-pvc.asp>
- Huang, B., Mohammad, M., Wathugala, W. *Application of a Temperature Dependent Viscoplastic Hierarchical Single Surface Model for Asphalt Mixtures*. Journal of Materials in Civil Engineering (ASCE). Volume 16, No. 2. April 1, 2004.
- Loomans, M., Oversloot, H., Bondt, A., Jansen, R., Rij, H., TNO Building and Construction Research, Ooms Avenhorn Holding B.V., TipSpit. *Design Tool for the Thermal Energy Potential of Asphalt Pavement*. Eight International IBPSA Conference. Netherlands: Eindhoven. August 2003.
- Mallick, R.B., Chen, B., Bhowmick, S. *Harvesting energy from asphalt pavements and reducing the heat island effect*. International Journal of Sustainable Engineering. Volume 2, No. 3. September 2009, Pages 214-228

Mamlouk, M. S., Wiczak, M.W., Kaloush, K.E., Hasan, N. *Determination of Thermal Properties of Asphalt Mixtures*. Journal of Testing and Evaluation. Volume 33, No. 2. March 2005. Pages 118-126

Matweb. Borealis BorPEX™ ME 2510 Medium Density Polyethylene Compound for Crosslinked Pipes (Pex-B (Silane)). Retrieved on November 29, 2009 from <http://www.matweb.com/search/datasheet>

National Oceanic and Atmospheric Administration. *General Solar Position Calculations*. <http://www.noaa.gov>

Viljoen, A. W. 2001, *Estimating Asphalt temperatures from air temperatures and basic sky parameters*, Transportek, CSIR, South Africa

## Appendix A: Example Economic Analysis (Houston, Texas)

<b>Input:</b>			
<b>NOAA Input Data</b>		<b>Location</b>	
<b>YRMODAHRMN</b>	<b>Air Temperature (°F)</b>	Houston, TX	
200709010053	81	<b>Latitude (°):</b>	29.97
200709010153	79	<b>Longitude (°):</b>	95.28
200709010253	77	<b>Timezone:</b>	6
200709010353	75	<b>Pipe Material Properties</b>	
200709010453	75	<b>Material:</b>	Copper
200709010553	73	<b>Notes:</b>	CS12200 - Type K
200709010600	74	<b>Inner Diameter (in):</b>	0.745
200709010653	73	<b>Outer Diameter (in):</b>	0.875
200709010753	73	<b>Bend Coefficient, Kb:</b>	0.40
200709010853	73	<b>Maximum Run Length (m):</b>	50
200709010953	75	<b>Fluid Properties</b>	
200709011053	75	<b>k (W/(m*°C)):</b>	0.606
200709011153	75	<b>ρ (kg/m3):</b>	1000
200709011200	75	<b>cp (J/(kg*°C)):</b>	4181
200709011253	75	<b>Inlet fluid temperature (°C):</b>	20
200709011353	79	<b>Outlet tolerance (&gt;0) (C°):</b>	1
200709011453	77	<b>Viscosity ((N*sec)/m2):</b>	0.00089
200709011553	84	<b>Efficiencies</b>	
200709011653	86	<b>Pump (%):</b>	100.0%
200709011753	86	<b>Pavement to Fluid (%):</b>	100.0%
200709011800	86	<b>Extra pipe length (m):</b>	0
200709011853	90	<b>Costs</b>	
200709011953	91	<b>Unit Length (\$/m)</b>	
200709012053	88	<b>Pipe Material:</b>	\$7.00
200709012153	90	<b>Other:</b>	\$0.00
200709012253	88	<b>Capital Costs</b>	
200709012353	86	<b>Pipe Supports:</b>	\$5,000.00
200709020000	86	<b>Monitoring System:</b>	\$5,000.00
200709020053	82	<b>Pump:</b>	\$500.00
200709020253	75	<b>Other:</b>	\$0.00
200709020353	73	<b>Maintenance (\$/yr)</b>	
200709020453	73	<b>Standard:</b>	\$1,000.00
200709020553	73	<b>Other:</b>	\$0.00
200709020600	74	<b>Electricity</b>	
200709020653	73	<b>Rate:</b>	\$0.05963
200709020753	73		
200709020853	73		
200709020953	73		
200709021053	73		

Figure 19: Example 'Input' worksheet

**Temperature Statistics:**

<b>Maximum Air Temperature (°C)</b>												
<b>Day of Month</b>	<b>January</b>	<b>February</b>	<b>March</b>	<b>April</b>	<b>May</b>	<b>June</b>	<b>July</b>	<b>August</b>	<b>September</b>	<b>October</b>	<b>November</b>	<b>December</b>
1	16.11	15.00	26.11	27.78	28.89	32.78	32.78	36.11	32.78	32.78	27.78	22.78
2	10.00	22.78	23.33	26.11	31.11	31.11	32.78	37.22	30.00	32.22	27.78	26.11
3	7.78	27.22	22.22	27.22	28.89	35.00	33.89	36.67	32.22	32.22	27.78	22.22
4	17.22	26.11	17.22	28.89	27.78	32.78	33.33	37.22	26.11	32.78	27.78	17.22
5	23.89	26.11	22.22	22.78	25.00	32.78	32.22	33.33	32.78	30.00	27.78	23.89
6	26.11	24.44	22.22	27.22	27.22	32.78	33.89	32.22	32.22	31.11	23.89	21.11
7	26.11	21.11	11.11	27.78	28.33	32.78	33.89	35.00	33.89	31.11	18.33	27.22
8	24.44	23.89	16.11	27.78	31.11	33.89	33.89	36.11	32.78	32.22	23.89	27.22
9	20.00	23.89	22.22	26.11	32.78	33.89	33.89	33.89	32.22	33.89	28.89	27.22
10	22.22	22.78	20.00	26.11	32.22	32.78	33.89	36.11	33.89	30.00	28.33	22.78
11	17.78	23.89	21.11	27.78	30.00	33.89	36.11	35.00	33.89	31.11	28.33	27.22
12	22.22	22.22	23.89	24.44	26.11	34.44	36.11	32.22	28.89	28.89	27.78	24.44
13	17.78	17.22	22.78	22.78	28.33	33.89	35.00	32.22	31.11	28.89	28.89	15.00
14	17.78	22.22	31.11	21.11	27.78	33.33	37.22	35.00	33.89	27.78	30.00	17.78
15	15.00	22.22	31.11	22.22	27.78	35.00	36.11	32.22	32.78	31.11	25.00	22.22
16	12.22	22.22	27.22	25.00	25.56	37.22	37.22	28.89	32.22	27.78	22.22	12.22
17	12.22	22.22	27.22	26.11	23.33	35.00	35.00	32.22	32.78	32.22	23.33	13.89
18	9.44	18.89	26.11	23.33	31.11	37.22	34.44	27.22	32.78	32.22	22.78	22.78
19	11.11	20.00	22.78	27.78	31.11	33.33	36.11	27.22	32.78	30.00	25.00	23.89
20	10.00	22.78	22.78	27.22	35.00	37.22	36.11	28.89	32.22	31.11	26.11	26.11
21	12.22	23.89	23.89	28.89	33.89	37.22	37.22	31.11	32.22	28.89	28.89	22.78
22	21.11	22.22	26.11	28.89	32.22	36.11	36.11	32.22	33.89	25.56	23.89	22.78
23	13.89	21.11	22.78	30.00	32.22	36.11	32.22	32.78	32.22	21.11	11.11	17.78
24	8.89	27.22	20.00	28.89	32.22	31.11	27.78	32.78	32.78	26.11	10.00	16.11
25	8.33	27.22	22.78	27.22	32.78	35.00	33.89	33.89	31.11	21.11	8.89	16.11
26	17.78	23.89	24.44	27.78	33.89	32.22	36.11	33.89	32.78	22.78	16.11	18.89
27	17.22	17.22	27.22	26.11	33.89	33.89	36.11	33.89	32.78	23.89	16.11	12.78
28	22.22	21.11	26.11	23.89	32.78	32.78	36.11	32.78	32.78	23.89	22.22	17.22
29	23.89		27.78	27.22	31.11	33.89	36.11	32.78	32.22	23.89	22.78	12.78
30	18.89		27.22	27.78	31.11	32.78	36.11	31.11	31.11	25.00	23.89	21.11
31	17.22		27.78		32.78		37.22	33.89		27.22		22.78
<b>Monthly Mean Air Temperature (°C)</b>												
<b>Month</b>	<b>January</b>	<b>February</b>	<b>March</b>	<b>April</b>	<b>May</b>	<b>June</b>	<b>July</b>	<b>August</b>	<b>September</b>	<b>October</b>	<b>November</b>	<b>December</b>
<b>Temperature</b>	11.78	16.23	17.89	20.89	25.76	28.87	29.12	28.74	27.32	22.80	18.18	14.97

Figure 20: Example 'Statistics' worksheet (continued on following pages)

Minimum Air Temperature (°C)												
Day of Month	January	February	March	April	May	June	July	August	September	October	November	December
1	5.00	1.11	12.78	22.22	21.67	22.78	22.22	23.89	22.78	23.89	15.00	15.56
2	1.11	6.11	13.89	20.00	22.78	23.89	22.22	25.56	22.78	21.67	15.00	21.11
3	2.78	17.78	8.89	21.11	20.00	25.00	21.11	26.11	23.89	18.89	16.11	7.22
4	0.56	21.11	2.78	13.89	12.78	26.11	22.22	22.22	22.22	20.00	13.89	1.11
5	12.78	22.22	3.89	12.22	17.22	26.67	22.22	22.78	25.00	22.78	16.11	6.11
6	17.78	3.89	7.78	11.11	16.67	26.67	22.78	23.89	23.89	25.00	16.11	8.89
7	18.89	2.78	2.78	13.89	21.67	26.11	22.78	23.89	23.89	23.89	12.22	12.78
8	16.11	3.89	2.22	18.89	22.78	25.56	23.89	25.56	23.89	22.78	10.00	22.22
9	7.22	11.67	6.11	18.89	21.11	26.11	22.78	23.89	23.89	22.78	17.78	21.11
10	13.89	12.78	12.78	17.78	22.78	22.78	22.78	26.11	23.89	21.67	16.67	13.89
11	3.89	11.67	11.11	21.11	22.78	22.78	23.89	26.67	22.78	17.22	16.11	22.22
12	3.89	12.22	7.22	12.78	15.00	22.78	23.89	27.78	22.78	17.22	17.78	12.22
13	7.78	2.78	10.00	7.78	22.22	23.89	22.78	26.11	23.89	16.11	17.78	7.22
14	2.78	6.11	20.00	6.67	22.78	22.78	25.56	25.00	22.78	17.22	21.67	12.78
15	7.78	15.00	16.11	6.11	18.89	22.78	23.89	25.00	22.78	17.78	12.78	7.78
16	7.78	17.78	12.22	8.89	17.22	23.89	23.89	22.78	20.00	17.78	3.89	1.67
17	7.22	10.00	20.00	17.78	15.00	25.00	22.78	22.78	18.89	22.78	12.78	1.11
18	3.89	7.22	22.78	12.78	13.89	21.67	22.22	27.22	21.11	23.89	16.67	10.00
19	2.78	5.00	12.22	8.89	13.89	22.78	22.78	22.78	23.89	15.56	17.22	11.11
20	2.22	11.67	6.11	10.56	22.78	22.22	22.78	22.78	21.11	13.89	18.89	20.00
21	3.89	17.78	7.78	21.11	22.78	22.78	25.00	23.89	18.89	17.22	18.89	6.11
22	11.67	11.11	12.22	22.22	26.11	22.78	23.89	23.89	18.89	13.89	6.11	12.78
23	6.11	6.11	13.89	18.89	26.11	22.78	23.89	23.89	22.78	10.56	7.22	0.00
24	3.89	12.78	7.22	22.22	26.67	22.22	23.89	22.78	21.11	10.00	6.11	1.11
25	3.89	10.00	7.78	22.22	26.11	23.89	22.78	25.00	22.78	10.00	7.22	1.11
26	3.89	11.11	17.78	20.00	25.00	22.22	26.11	23.89	22.78	6.67	3.89	7.22
27	6.11	2.22	17.78	17.78	22.78	22.78	23.89	23.89	22.78	8.89	3.89	1.11
28	5.00	3.89	17.78	11.67	22.22	22.78	23.89	23.89	22.78	11.11	6.11	10.00
29	18.89		17.78	7.78	21.11	22.78	22.78	23.89	20.56	11.11	10.00	5.00
30	1.11		22.22	13.89	21.11	22.78	25.56	23.89	23.89	10.56	11.11	2.78
31	8.89		20.00		28.89		25.56	23.89		12.22		2.78

<b>Maximum Asphalt Surface Temperature (°C)</b>												
<b>Day of Month</b>	<b>January</b>	<b>February</b>	<b>March</b>	<b>April</b>	<b>May</b>	<b>June</b>	<b>July</b>	<b>August</b>	<b>September</b>	<b>October</b>	<b>November</b>	<b>December</b>
1	37.27	20.93	50.06	44.58	46.32	33.52	53.31	48.66	51.33	33.39	51.52	23.52
2	14.93	47.02	46.56	49.55	42.29	31.13	51.76	56.35	53.22	33.71	46.66	26.12
3	12.26	48.18	38.64	50.98	32.61	35.29	51.06	61.05	58.70	41.45	39.23	22.64
4	33.00	40.84	19.04	46.52	28.05	34.16	48.43	64.10	30.83	52.16	32.19	19.00
5	37.22	33.68	23.10	31.32	25.21	35.91	45.02	59.09	44.07	53.78	28.18	27.75
6	36.77	26.40	23.15	28.75	32.30	38.09	44.24	53.39	35.13	56.85	24.66	27.50
7	33.99	21.12	12.97	28.16	39.84	40.52	41.73	49.27	33.93	49.51	23.55	36.35
8	29.64	26.50	20.30	33.44	50.98	44.14	39.30	43.14	37.07	40.53	35.92	39.10
9	22.83	32.83	45.68	40.55	57.88	46.60	37.11	35.58	45.70	35.02	47.72	41.68
10	23.27	39.43	43.68	48.14	59.17	47.80	35.35	36.14	56.58	30.74	51.73	39.55
11	17.87	46.56	38.35	52.23	52.80	51.00	36.44	37.76	60.81	38.60	52.72	45.98
12	22.43	46.66	31.75	44.98	44.46	53.38	36.12	41.36	50.53	44.72	49.45	44.83
13	19.30	38.28	23.83	35.19	40.76	54.39	35.67	49.31	46.10	51.77	45.13	36.68
14	21.84	36.07	32.03	25.35	34.34	55.13	39.61	58.85	39.19	51.95	39.78	40.43
15	22.66	28.08	39.20	22.34	29.93	57.85	41.25	59.13	32.94	52.12	29.10	45.58
16	24.21	22.90	44.00	26.99	25.58	60.90	46.02	51.61	34.69	38.20	22.88	18.18
17	28.73	23.00	50.75	34.94	23.51	59.32	48.07	50.89	43.76	35.23	23.52	19.93
18	14.58	25.13	49.70	40.59	35.15	62.02	51.99	29.55	53.71	32.24	25.38	47.11
19	16.96	34.61	39.70	51.05	40.19	58.47	57.80	27.91	59.43	33.58	32.18	48.32
20	16.12	44.67	30.27	51.37	49.83	62.58	61.04	28.90	57.09	43.77	38.87	50.59
21	35.66	48.37	24.77	48.48	54.08	62.71	63.95	33.64	48.79	48.66	46.99	47.27
22	41.35	43.20	27.12	40.68	56.52	61.65	62.79	41.91	40.38	49.83	46.04	47.27
23	29.26	34.14	30.56	34.25	58.79	61.60	56.85	51.32	32.63	26.84	17.18	42.27
24	11.32	31.86	37.18	29.11	59.03	56.48	32.49	58.02	34.63	42.55	16.05	40.60
25	9.46	27.38	46.45	28.54	57.93	60.14	49.39	60.64	41.10	23.12	14.43	40.57
26	18.72	25.92	47.90	34.70	55.89	57.02	45.89	56.15	52.92	23.19	20.77	43.29
27	17.29	26.57	43.90	40.75	51.78	58.22	40.73	47.59	59.22	24.05	19.69	18.84
28	24.49	39.38	33.45	45.22	46.19	56.47	37.19	37.76	58.05	27.98	32.05	41.26
29	31.05		28.64	51.66	40.20	56.76	36.13	33.01	49.51	35.47	28.59	18.69
30	32.44		28.19	50.66	36.47	54.60	37.95	32.92	38.23	44.29	26.59	44.19
31	36.90		35.33		35.31		43.54	42.96		51.18		45.04

<b>Maximum Asphalt Surface Temperature (°C)</b>												
<b>Day of Month</b>	<b>January</b>	<b>February</b>	<b>March</b>	<b>April</b>	<b>May</b>	<b>June</b>	<b>July</b>	<b>August</b>	<b>September</b>	<b>October</b>	<b>November</b>	<b>December</b>
1	9.65	6.19	16.57	24.98	24.48	25.47	24.98	26.46	25.47	26.46	18.55	19.04
2	6.19	10.64	17.56	23.00	25.47	26.46	24.98	27.94	25.47	24.48	18.55	23.99
3	2.73	21.02	13.11	23.99	23.00	27.45	23.99	28.44	26.46	22.01	19.54	11.63
4	5.69	23.99	7.67	17.56	16.57	28.44	24.98	24.98	24.98	23.00	17.56	6.19
5	16.57	24.98	8.66	16.08	20.53	28.93	24.98	25.47	27.45	25.47	19.54	10.64
6	21.02	8.66	12.12	15.09	20.03	28.93	25.47	26.46	26.46	27.45	19.54	13.11
7	22.01	7.67	7.67	17.56	24.48	28.44	25.47	26.46	26.46	26.46	16.08	16.57
8	19.54	8.66	7.18	22.01	25.47	27.94	26.46	27.94	26.46	25.47	14.10	24.98
9	11.63	15.58	10.64	22.01	23.99	28.44	25.47	26.46	26.46	25.47	21.02	23.99
10	17.56	16.57	16.57	21.02	25.47	25.47	25.47	28.44	26.46	24.48	20.03	17.56
11	8.66	15.58	15.09	23.99	25.47	25.47	26.46	28.93	25.47	20.53	19.54	24.98
12	8.66	16.08	11.63	16.57	18.55	25.47	26.46	29.92	25.47	20.53	21.02	16.08
13	12.12	7.67	14.10	12.12	24.98	26.46	25.47	28.44	26.46	19.54	21.02	11.63
14	7.67	10.64	23.00	11.13	25.47	25.47	27.94	27.45	25.47	20.53	24.48	16.57
15	12.12	18.55	19.54	10.64	22.01	25.47	26.46	27.45	25.47	21.02	16.57	12.12
16	12.12	21.02	16.08	13.11	20.53	26.46	26.46	25.47	23.00	21.02	8.66	6.68
17	11.63	14.10	23.00	21.02	18.55	27.45	25.47	25.47	22.01	25.47	16.57	4.21
18	8.66	11.63	25.47	16.57	17.56	24.48	24.98	29.43	23.99	26.46	20.03	14.10
19	7.67	9.65	16.08	13.11	17.56	25.47	25.47	25.47	26.46	19.04	20.53	15.09
20	3.22	15.58	10.64	14.59	25.47	24.98	25.47	25.47	23.99	17.56	22.01	23.00
21	8.66	21.02	12.12	23.99	25.47	25.47	27.45	26.46	22.01	20.53	22.01	10.64
22	15.58	15.09	16.08	24.98	28.44	25.47	26.46	26.46	22.01	17.56	10.64	16.57
23	10.64	10.64	17.56	22.01	28.44	25.47	26.46	26.46	25.47	14.59	11.63	5.20
24	8.66	16.57	11.63	24.98	28.93	24.98	26.46	25.47	23.99	14.10	10.64	6.19
25	8.66	14.10	12.12	24.98	28.44	26.46	25.47	27.45	25.47	14.10	11.63	6.19
26	8.66	15.09	21.02	23.00	27.45	24.98	28.44	26.46	25.47	11.13	8.66	11.63
27	10.64	7.18	21.02	21.02	25.47	25.47	26.46	26.46	25.47	13.11	8.66	6.19
28	9.65	8.66	21.02	15.58	24.98	25.47	26.46	26.46	25.47	15.09	10.64	14.10
29	22.01		21.02	12.12	23.99	25.47	25.47	26.46	23.49	15.09	14.10	9.65
30	6.19		24.98	17.56	23.99	25.47	27.94	26.46	26.46	14.59	15.09	7.67
31	13.11		23.00		30.91		27.94	26.46		16.08		7.67

<b>Temperature Profile:</b>												
<b>Month</b>	<b>Day</b>	<b>Hour</b>	<b>Day of Year</b>	<b>Hour of Year</b>	<b>Temperature (°C) at Depth (mm)</b>							
					<b>Surface</b>	<b>25</b>	<b>50</b>	<b>75</b>	<b>100</b>	<b>125</b>	<b>150</b>	
January	1	0	1	0	13.86	15.01	15.81	16.43	16.93	17.30	17.52	
January	1	1	1	1	12.91	14.00	14.80	15.45	15.98	16.40	16.68	
January	1	2	1	2	12.18	13.22	14.02	14.69	15.24	15.69	16.02	
January	1	3	1	3	11.61	12.61	13.42	14.10	14.67	15.15	15.52	
January	1	4	1	4	11.16	12.14	12.95	13.64	14.23	14.73	15.13	
January	1	5	1	5	10.82	11.78	12.59	13.29	13.89	14.41	14.82	
January	1	6	1	6	10.56	11.50	12.31	13.01	13.63	14.16	14.59	
January	1	7	1	7	10.35	11.28	12.09	12.80	13.42	13.96	14.41	
January	1	8	1	8	10.19	11.11	11.92	12.63	13.26	13.81	14.27	
January	1	9	1	9	11.38	11.88	12.42	12.97	13.49	13.95	14.35	
January	1	10	1	10	18.91	17.77	17.18	16.92	16.86	16.86	16.84	
January	1	11	1	11	25.72	23.18	21.60	20.64	20.05	19.63	19.22	
January	1	12	1	12	31.29	27.77	25.45	23.94	22.94	22.17	21.43	
January	1	13	1	13	35.18	31.23	28.51	26.67	25.39	24.38	23.39	
January	1	14	1	14	37.09	33.33	30.61	28.69	27.31	26.17	25.03	
January	1	15	1	15	36.88	33.95	31.63	29.91	28.61	27.48	26.29	
January	1	16	1	16	34.56	33.03	31.52	30.26	29.24	28.27	27.14	
January	1	17	1	17	30.30	30.64	30.27	29.73	29.17	28.50	27.55	
January	1	18	1	18	24.98	26.36	26.75	26.77	26.61	26.26	25.61	
January	1	19	1	19	20.74	22.01	22.49	22.67	22.69	22.56	22.16	
January	1	20	1	20	17.45	18.64	19.20	19.50	19.66	19.68	19.49	
January	1	21	1	21	14.91	16.03	16.64	17.04	17.31	17.46	17.42	
January	1	22	1	22	12.94	14.01	14.67	15.14	15.50	15.74	15.82	
January	1	23	1	23	11.42	12.44	13.14	13.67	14.09	14.41	14.58	
January	2	0	2	24	10.25	11.24	11.96	12.53	13.01	13.38	13.63	
January	2	1	2	25	9.33	10.30	11.04	11.65	12.16	12.58	12.88	
January	2	2	2	26	8.62	9.57	10.33	10.96	11.51	11.96	12.30	
January	2	3	2	27	8.07	9.01	9.77	10.43	11.00	11.48	11.86	
January	2	4	2	28	7.65	8.57	9.35	10.02	10.61	11.11	11.51	
January	2	5	2	29	7.32	8.23	9.02	9.70	10.30	10.82	11.24	
January	2	6	2	30	7.06	7.97	8.76	9.46	10.07	10.60	11.04	
January	2	7	2	31	6.87	7.77	8.56	9.26	9.89	10.42	10.87	
January	2	8	2	32	6.71	7.61	8.41	9.12	9.74	10.29	10.75	
January	2	9	2	33	6.73	7.44	8.13	8.78	9.37	9.90	10.35	
January	2	10	2	34	9.11	9.08	9.26	9.54	9.88	10.20	10.48	
January	2	11	2	35	11.26	10.59	10.31	10.26	10.35	10.49	10.61	
January	2	12	2	36	13.03	11.87	11.22	10.90	10.78	10.76	10.73	

Figure 21: Example 'Profile' worksheet

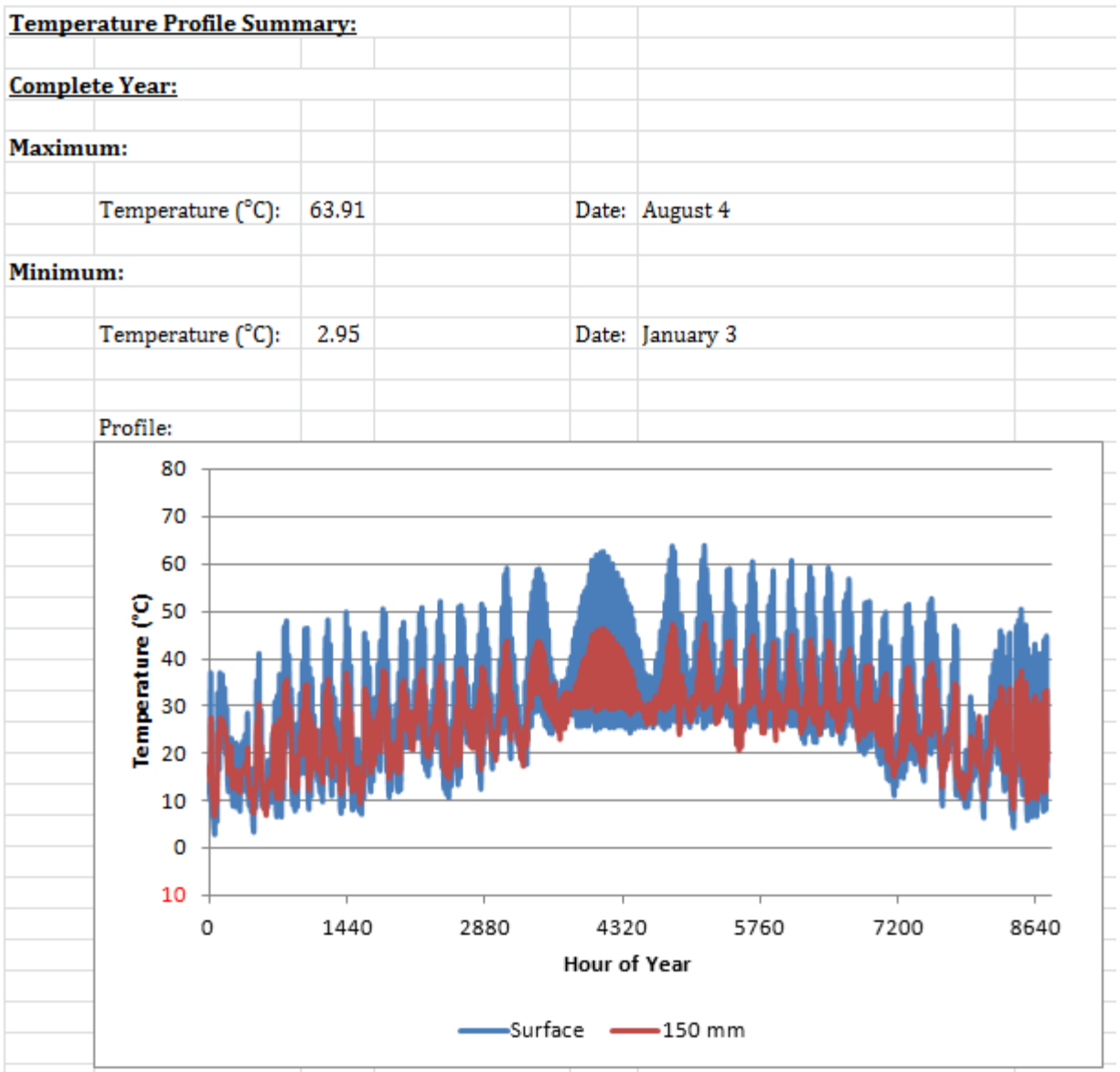


Figure 22: Example 'Profile Summary' Worksheet (continued on the next page)

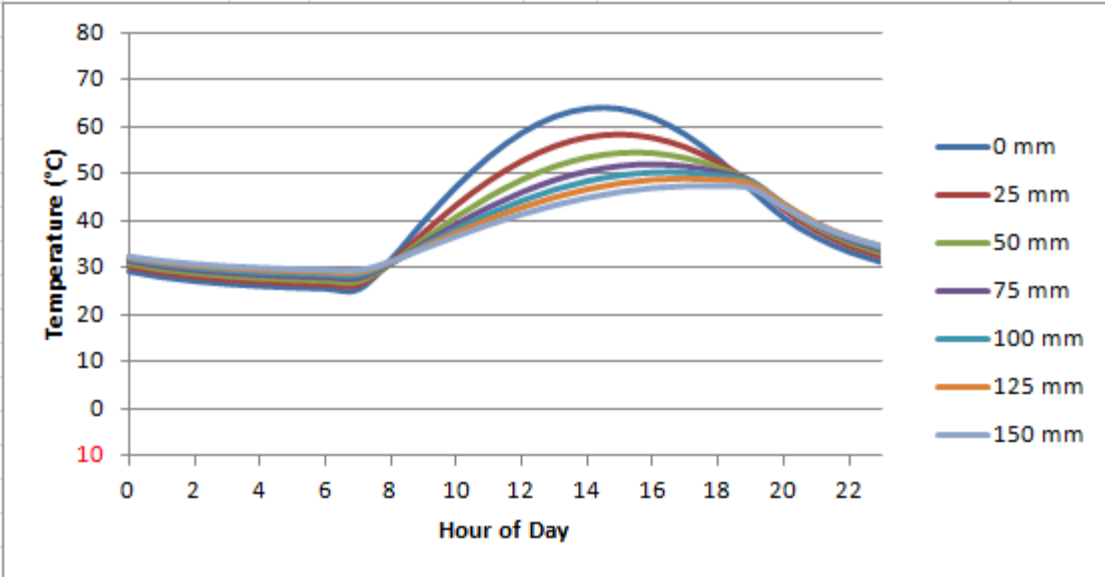
**50 mm Depth Temperature:**

**Maximum:**

Temperature (°C): 54.46

Date: August 4

**Profile:**

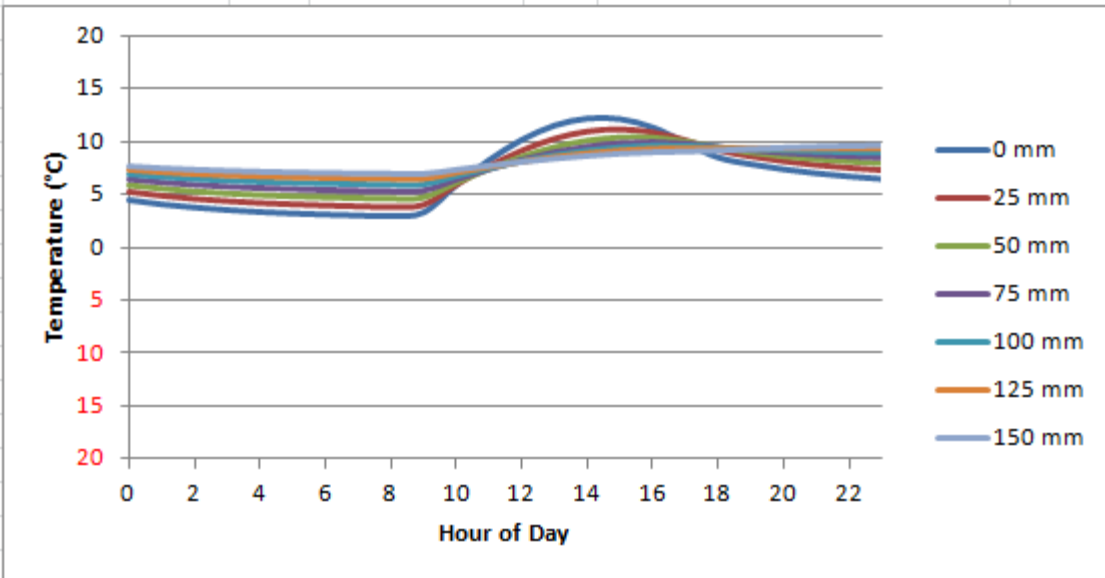


**Minimum:**

Temperature (°C): 4.61

Date: January 3

**Profile:**



Pipe Material Properties		Location			Fluid Properties				
Material:	Copper	<b>Houston, TX</b>			k (W/(m <sup>2</sup> C)):	0.606			
Notes:	CS12200 - Type K				Latitude (°):	29.97	ρ (kg/m <sup>3</sup> ):	1000	
Inner Diameter (in):	0.745				Longitude (°):	95.28	c <sub>p</sub> (J/(kg°C)):	4181	
Outer Diameter (in):	0.875				Timezone:	6	Inlet fluid temperature (°C):	20	
Bend Coefficient, Kb:	0.4				Electricity Rate (\$/kWh):	\$0.05960	Outlet tolerance (C°):	1	
Maximum Run Length (m):	50						Viscosity ((N*sec)/m <sup>2</sup> ):	0.00089	
Efficiencies		Depth			Costs				
Pump (%):	100.0%	<b>0 mm</b>			Per Length (\$/m):	\$7.00			
Pavement to Fluid (%):	100.0%				Maintenance (\$/yr):	\$1,000.00			
Extra pipe length (m):	0.0%				Other Capital Cost (\$):	\$10,500.00			
Flowrate (L/min)	Network Length (m)	Pump Power (hp)	Grid Consumption (kWh)	Energy Harvested (kWh)	Initial Cost	Yearly Savings	Payback Period (years)		
1	38	0.00	0	5686	\$10,764.76	\$661.10	16.3		
2	76	0.00	0	11373	\$11,029.52	\$322.21	34.2		
3	113	0.00	2	17059	\$11,294.27	\$16.62	679.7		
4	151	0.00	5	22745	\$11,559.03	\$355.33	32.5		
5	189	0.00	11	28432	\$11,823.79	\$693.85	17.0		
6	227	0.00	23	34118	\$12,088.55	\$1,032.08	11.7		
7	265	0.01	40	39804	\$12,353.31	\$1,369.93	9.0		
8	303	0.01	67	45491	\$12,618.06	\$1,707.26	7.4		
9	340	0.02	104	51177	\$12,882.82	\$2,043.96	6.3		
10	378	0.02	154	56863	\$13,147.58	\$2,379.87	5.5		
11	416	0.03	221	62550	\$13,412.34	\$2,714.81	4.9		
12	454	0.05	306	68236	\$13,677.09	\$3,048.65	4.5		
13	492	0.06	412	73922	\$13,941.85	\$3,381.19	4.1		
14	530	0.08	545	79609	\$14,206.61	\$3,712.17	3.8		
15	567	0.11	706	85295	\$14,471.37	\$4,041.50	3.6		
16	605	0.13	861	90981	\$14,736.13	\$4,371.15	3.4		
17	643	0.17	1084	96668	\$15,000.88	\$4,696.80	3.2		
18	681	0.21	1346	102354	\$15,265.64	\$5,020.07	3.0		
19	719	0.25	1655	108040	\$15,530.40	\$5,340.56	2.9		
20	756	0.31	2010	113727	\$15,795.16	\$5,658.29	2.8		
21	794	0.37	2419	119413	\$16,059.91	\$5,972.85	2.7		
22	832	0.44	2890	125099	\$16,324.67	\$6,283.69	2.6		
23	870	0.52	3420	130786	\$16,589.43	\$6,590.98	2.5		
24	908	0.62	4025	136472	\$16,854.19	\$6,893.86	2.4		
25	946	0.72	4698	142158	\$17,118.95	\$7,192.63	2.4		
26	983	0.83	5451	147845	\$17,383.70	\$7,486.66	2.3		
27	1021	0.96	6298	153531	\$17,648.46	\$7,775.12	2.3		
28	1059	1.11	7228	159217	\$17,913.22	\$8,058.56	2.2		
29	1097	1.26	8256	164904	\$18,177.98	\$8,336.18	2.2		
30	1135	1.44	9400	170590	\$18,442.74	\$8,606.95	2.1		

Figure 23: Example 'Results' worksheet (continued on the next page)

Pipe Material Properties			Location		Fluid Properties			
Material:	Copper		<b>Houston, TX</b>		k (W/(m <sup>2</sup> C)):	0.606		
Notes:	CS12200 - Type K				ρ (kg/m <sup>3</sup> ):	1000		
Inner Diameter (in):	0.745				c <sub>p</sub> (J/(kg <sup>o</sup> C)):	4181		
Outer Diameter (in):	0.875				Inlet fluid temperature (°C):	20		
Bend Coefficient, Kb:	0.4				Outlet tolerance (C°):	1		
Maximum Run Length (m):	50		Electricity Rate (\$/kWh):	\$0.05960		Viscosity ((N*sec)/m <sup>2</sup> ):	0.00089	
Efficiencies			Depth		Costs			
Pump (%):	100.0%		<b>25 mm</b>		Pipe (\$/m):	\$7.00		
Pavement to Fluid (%):	100.0%				Maintenance (\$/yr):	\$1,000.00		
Extra pipe length (m):	0.0%				Other Capital Cost (\$):	\$10,500.00		
Flowrate (L/min)	Network Length (m)	Pump Power (hp)	Grid Consumption (kWh)	Energy Harnessed (kWh)	Initial Cost	Yearly Savings	Payback Period (years)	
1	36	0.00	0	5272	\$10,755.38	\$685.80	15.7	
2	73	0.00	0	10544	\$11,010.77	\$371.61	29.6	
3	109	0.00	2	15816	\$11,266.15	\$57.49	196.0	
4	146	0.00	5	21087	\$11,521.53	\$256.53	44.9	
5	182	0.00	11	26359	\$11,776.91	\$570.36	20.6	
6	219	0.00	22	31631	\$12,032.30	\$883.92	13.6	
7	255	0.01	39	36903	\$12,287.68	\$1,197.10	10.3	
8	292	0.01	64	42175	\$12,543.06	\$1,509.80	8.3	
9	328	0.02	100	47447	\$12,798.45	\$1,821.86	7.0	
10	365	0.02	149	52719	\$13,053.83	\$2,133.17	6.1	
11	401	0.03	213	57991	\$13,309.21	\$2,443.54	5.4	
12	438	0.05	295	63262	\$13,564.60	\$2,752.86	4.9	
13	474	0.06	398	68534	\$13,819.98	\$3,060.93	4.5	
14	511	0.08	526	73806	\$14,075.36	\$3,367.48	4.2	
15	547	0.10	681	79078	\$14,330.74	\$3,672.44	3.9	
16	584	0.13	829	84350	\$14,586.13	\$3,977.82	3.7	
17	620	0.16	1046	89622	\$14,841.51	\$4,279.12	3.5	
18	657	0.20	1299	94894	\$15,096.89	\$4,578.24	3.3	
19	693	0.24	1594	100165	\$15,352.28	\$4,874.83	3.1	
20	730	0.30	1940	105437	\$15,607.66	\$5,168.44	3.0	
21	766	0.36	2334	110709	\$15,863.04	\$5,459.15	2.9	
22	803	0.43	2789	115981	\$16,118.42	\$5,746.26	2.8	
23	839	0.51	3300	121253	\$16,373.81	\$6,029.97	2.7	
24	876	0.59	3878	126525	\$16,629.19	\$6,309.73	2.6	
25	912	0.69	4534	131797	\$16,884.57	\$6,584.87	2.6	
26	949	0.81	5260	137069	\$17,139.96	\$6,855.77	2.5	
27	985	0.93	6069	142340	\$17,395.34	\$7,121.76	2.4	
28	1022	1.07	6975	147612	\$17,650.72	\$7,381.96	2.4	
29	1058	1.22	7968	152884	\$17,906.11	\$7,637.03	2.3	
30	1094	1.39	9060	158156	\$18,161.49	\$7,886.12	2.3	

		<b>Location</b>			
<b>Pipe Material Properties</b>		<b>Houston, TX</b>		<b>Fluid Properties</b>	
Material:	Copper			k (W/(m <sup>2</sup> C)):	0.606
Notes:	CS12200 - Type K			ρ (kg/m <sup>3</sup> ):	1000
Inner Diameter (in):	0.745			c <sub>p</sub> (J/(kg <sup>o</sup> C)):	4181
Outer Diameter (in):	0.875			Inlet fluid temperature (°C):	20
Bend Coefficient, Kb:	0.4			Outlet tolerance (C°):	1
Maximum Run Length (m):	50	Electricity Rate (\$/kWh):	\$0.05960	Viscosity ((N*sec)/m <sup>2</sup> ):	0.00089
<b>Efficiencies</b>		<b>Depth</b>		<b>Costs</b>	
Pump (%):	100.0%	<b>50 mm</b>		Pipe (\$/m):	\$7.00
Pavement to Fluid (%):	100.0%			Maintenance (\$/yr):	\$1,000.00
Extra pipe length (m):	0.0%			Other Capital Cost (\$):	\$10,500.00

Flowrate (L/min)	Network Length (m)	Pump Power (hp)	Grid Consumption (kWh)	Energy Harvested (kWh)	Initial Cost	Yearly Savings	Payback Period (years)
1	35	0.00	0	4981	\$10,747.79	\$703.12	15.3
2	71	0.00	0	9963	\$10,995.58	\$406.26	27.1
3	106	0.00	2	14944	\$11,243.38	\$109.45	102.7
4	142	0.00	5	19925	\$11,491.17	\$187.25	61.4
5	177	0.00	11	24906	\$11,738.96	\$483.78	24.3
6	212	0.00	21	29888	\$11,986.75	\$780.03	15.4
7	248	0.01	38	34869	\$12,234.55	\$1,075.92	11.4
8	283	0.01	62	39850	\$12,482.34	\$1,371.34	9.1
9	319	0.01	97	44831	\$12,730.13	\$1,666.15	7.6
10	354	0.02	144	49813	\$12,977.92	\$1,960.23	6.6
11	389	0.03	206	54794	\$13,225.71	\$2,253.42	5.9
12	425	0.04	286	59775	\$13,473.51	\$2,545.53	5.3
13	460	0.06	386	64756	\$13,721.30	\$2,836.45	4.8
14	496	0.08	510	69738	\$13,969.09	\$3,125.98	4.5
15	531	0.10	661	74719	\$14,216.88	\$3,413.83	4.2
16	566	0.12	805	79700	\$14,464.68	\$3,702.14	3.9
17	602	0.16	1015	84681	\$14,712.47	\$3,986.50	3.7
18	637	0.19	1261	89663	\$14,960.26	\$4,268.75	3.5
19	673	0.24	1548	94644	\$15,208.05	\$4,548.53	3.3
20	708	0.29	1883	99625	\$15,455.84	\$4,825.42	3.2
21	743	0.35	2266	104606	\$15,703.64	\$5,099.50	3.1
22	779	0.41	2703	109588	\$15,951.43	\$5,370.35	3.0
23	814	0.49	3204	114569	\$16,199.22	\$5,637.37	2.9
24	850	0.58	3764	119550	\$16,447.01	\$5,900.83	2.8
25	885	0.67	4394	124531	\$16,694.81	\$6,160.16	2.7
26	920	0.78	5106	129513	\$16,942.60	\$6,414.63	2.6
27	956	0.90	5891	134494	\$17,190.39	\$6,664.72	2.6
28	991	1.04	6762	139475	\$17,438.18	\$6,909.71	2.5
29	1027	1.18	7734	144456	\$17,685.97	\$7,148.66	2.5
30	1062	1.35	8794	149438	\$17,933.77	\$7,382.35	2.4

Pipe Material Properties		Location		Fluid Properties	
Material:	Copper	<b>Houston, TX</b>		k (W/(m <sup>2</sup> C)):	0.606
Notes:	CS12200 - Type K			ρ (kg/m <sup>3</sup> ):	1000
Inner Diameter (in):	0.745			Latitude (°):	29.97
Outer Diameter (in):	0.875			Longitude (°):	95.28
Bend Coefficient, Kb:	0.4			Timezone:	6
Maximum Run Length (m):	50	Electricity Rate (\$/kWh):	\$0.05960	Inlet fluid temperature (°C):	20
Efficiencies		Depth		Costs	
Pump (%):	100.0%	<b>75 mm</b>		Pipe (\$/m):	\$7.00
Pavement to Fluid (%):	100.0%			Maintenance (\$/yr):	\$1,000.00
Extra pipe length (m):	0.0%			Other Capital Cost (\$):	\$10,500.00

Flowrate (L/min)	Network Length (m)	Pump Power (hp)	Grid Consumption (kWh)	Energy Harnessed (kWh)	Initial Cost	Yearly Savings	Payback Period (years)
1	35	0.00	0	4812	\$10,742.74	\$713.21	15.1
2	69	0.00	0	9624	\$10,985.48	\$426.45	25.8
3	104	0.00	2	14436	\$11,228.22	\$139.73	80.4
4	139	0.00	5	19247	\$11,470.96	\$146.88	78.1
5	173	0.00	10	24059	\$11,713.70	\$433.31	27.0
6	208	0.00	21	28871	\$11,956.44	\$719.48	16.6
7	243	0.01	37	33683	\$12,199.18	\$1,005.30	12.1
8	277	0.01	61	38495	\$12,441.92	\$1,290.65	9.6
9	312	0.01	95	43307	\$12,684.66	\$1,575.40	8.1
10	347	0.02	141	48119	\$12,927.40	\$1,859.44	7.0
11	381	0.03	202	52930	\$13,170.14	\$2,142.62	6.1
12	416	0.04	280	57742	\$13,412.88	\$2,424.73	5.5
13	451	0.06	378	62554	\$13,655.62	\$2,705.68	5.0
14	485	0.08	499	67366	\$13,898.36	\$2,985.25	4.7
15	520	0.10	648	72178	\$14,141.10	\$3,263.19	4.3
16	555	0.12	789	76990	\$14,383.84	\$3,541.58	4.1
17	590	0.15	993	81802	\$14,626.58	\$3,816.21	3.8
18	624	0.19	1235	86613	\$14,869.32	\$4,088.54	3.6
19	659	0.23	1516	91425	\$15,112.06	\$4,358.58	3.5
20	694	0.28	1842	96237	\$15,354.80	\$4,625.96	3.3
21	728	0.34	2220	101049	\$15,597.54	\$4,890.22	3.2
22	763	0.41	2648	105861	\$15,840.28	\$5,151.49	3.1
23	798	0.48	3134	110673	\$16,083.02	\$5,409.31	3.0
24	832	0.56	3689	115485	\$16,325.76	\$5,663.05	2.9
25	867	0.66	4306	120297	\$16,568.50	\$5,913.05	2.8
26	902	0.77	5003	125108	\$16,811.24	\$6,158.27	2.7
27	936	0.88	5772	129920	\$17,053.98	\$6,399.21	2.7
28	971	1.01	6626	134732	\$17,296.72	\$6,635.15	2.6
29	1006	1.16	7578	139544	\$17,539.46	\$6,865.17	2.6
30	1040	1.32	8617	144356	\$17,782.20	\$7,090.04	2.5

Pipe Material Properties			Location		Fluid Properties			
Material:	Copper		<b>Houston, TX</b>		k (W/(m <sup>2</sup> C)):	0.606		
Notes:	CS12200 - Type K				ρ (kg/m <sup>3</sup> ):	1000		
Inner Diameter (in):	0.745				c <sub>p</sub> (J/(kg <sup>o</sup> C)):	4181		
Outer Diameter (in):	0.875				Inlet fluid temperature (°C):	20		
Bend Coefficient, Kb:	0.4				Outlet tolerance (C°):	1		
Maximum Run Length (m):	50		Electricity Rate (\$/kWh):	\$0.05960		Viscosity ((N <sup>o</sup> sec)/m <sup>2</sup> ):	0.00089	
Efficiencies			Depth		Costs			
Pump (%):	100.0%		<b>100 mm</b>		Pipe (\$/m):	\$7.00		
Pavement to Fluid (%):	100.0%				Maintenance (\$/yr):	\$1,000.00		
Extra pipe length (m):	0.0%				Other Capital Cost (\$):	\$10,500.00		
Flowrate (L/min)	Network Length (m)	Pump Power (hp)	Grid Consumption (kWh)	Energy Harnessed (kWh)	Initial Cost	Yearly Savings	Payback Period (years)	
1	34	0.00	0	4721	\$10,738.82	\$718.66	14.9	
2	68	0.00	0	9441	\$10,977.65	\$437.33	25.1	
3	102	0.00	2	14162	\$11,216.47	\$156.05	71.9	
4	136	0.00	4	18882	\$11,455.29	\$125.11	91.6	
5	171	0.00	10	23603	\$11,694.12	\$406.11	28.8	
6	205	0.00	20	28323	\$11,932.94	\$686.85	17.4	
7	239	0.01	36	33044	\$12,171.77	\$967.24	12.6	
8	273	0.01	60	37764	\$12,410.59	\$1,247.18	10.0	
9	307	0.01	94	42485	\$12,649.41	\$1,526.52	8.3	
10	341	0.02	139	47206	\$12,888.24	\$1,805.16	7.1	
11	375	0.03	199	51926	\$13,127.06	\$2,082.95	6.3	
12	409	0.04	276	56647	\$13,365.88	\$2,359.69	5.7	
13	444	0.06	372	61367	\$13,604.71	\$2,635.30	5.2	
14	478	0.08	491	66088	\$13,843.53	\$2,909.55	4.8	
15	512	0.10	638	70808	\$14,082.35	\$3,182.18	4.4	
16	546	0.12	776	75529	\$14,321.18	\$3,455.26	4.1	
17	580	0.15	977	80249	\$14,560.00	\$3,724.65	3.9	
18	614	0.19	1216	84970	\$14,798.82	\$3,991.76	3.7	
19	648	0.23	1492	89691	\$15,037.65	\$4,256.63	3.5	
20	682	0.28	1812	94411	\$15,276.47	\$4,518.88	3.4	
21	716	0.33	2185	99132	\$15,515.30	\$4,778.05	3.2	
22	751	0.40	2606	103852	\$15,754.12	\$5,034.29	3.1	
23	785	0.47	3084	108573	\$15,992.94	\$5,287.13	3.0	
24	819	0.56	3630	113293	\$16,231.77	\$5,535.95	2.9	
25	853	0.65	4237	118014	\$16,470.59	\$5,781.10	2.8	
26	887	0.75	4916	122735	\$16,709.41	\$6,021.97	2.8	
27	921	0.87	5680	127455	\$16,948.24	\$6,257.76	2.7	
28	955	1.00	6520	132176	\$17,187.06	\$6,489.08	2.6	
29	989	1.14	7447	136896	\$17,425.88	\$6,715.14	2.6	
30	1024	1.30	8480	141617	\$17,664.71	\$6,934.97	2.5	

Pipe Material Properties			Location		Fluid Properties			
Material:	Copper		<b>Houston, TX</b>		k (W/(m <sup>2</sup> C)):	0.606		
Notes:	CS12200 - Type K				ρ (kg/m <sup>3</sup> ):	1000		
Inner Diameter (in):	0.745				c <sub>p</sub> (J/(kg°C)):	4181		
Outer Diameter (in):	0.875				Inlet fluid temperature (°C):	20		
Bend Coefficient, Kb:	0.4				Outlet tolerance (C°):	1		
Maximum Run Length (m):	50		Electricity Rate (\$/kWh):	\$0.05960		Viscosity ((N*sec)/m <sup>2</sup> ):	0.00089	
Efficiencies			Depth		Costs			
Pump (%):	100.0%		<b>125 mm</b>		Pipe (\$/m):	\$7.00		
Pavement to Fluid (%):	100.0%				Maintenance (\$/yr):	\$1,000.00		
Extra pipe length (m):	0.0%				Other Capital Cost (\$):	\$10,500.00		
Flowrate (L/min)	Network Length (m)	Pump Power (hp)	Grid Consumption (kWh)	Energy Harnessed (kWh)	Initial Cost	Yearly Savings	Payback Period (years)	
1	34	0.00	0	4646	\$10,735.76	\$723.07	14.8	
2	67	0.00	0	9293	\$10,971.52	\$446.17	24.6	
3	101	0.00	2	13939	\$11,207.28	\$169.31	66.2	
4	135	0.00	4	18586	\$11,443.04	\$107.45	106.5	
5	168	0.00	10	23232	\$11,678.80	\$384.03	30.4	
6	202	0.00	20	27879	\$11,914.56	\$660.36	18.0	
7	236	0.01	36	32525	\$12,150.32	\$936.34	13.0	
8	269	0.01	59	37171	\$12,386.08	\$1,211.88	10.2	
9	303	0.01	93	41818	\$12,621.84	\$1,486.83	8.5	
10	337	0.02	137	46464	\$12,857.60	\$1,761.09	7.3	
11	370	0.03	196	51111	\$13,093.36	\$2,034.50	6.4	
12	404	0.04	272	55757	\$13,329.12	\$2,306.88	5.8	
13	438	0.06	368	60404	\$13,564.88	\$2,578.14	5.3	
14	472	0.07	485	65050	\$13,800.64	\$2,848.06	4.8	
15	505	0.10	630	69696	\$14,036.40	\$3,116.39	4.5	
16	539	0.12	766	74343	\$14,272.16	\$3,385.16	4.2	
17	573	0.15	964	78989	\$14,507.92	\$3,650.28	4.0	
18	606	0.18	1200	83636	\$14,743.68	\$3,913.15	3.8	
19	640	0.23	1473	88282	\$14,979.44	\$4,173.81	3.6	
20	674	0.27	1789	92929	\$15,215.20	\$4,431.89	3.4	
21	707	0.33	2157	97575	\$15,450.96	\$4,686.92	3.3	
22	741	0.39	2573	102221	\$15,686.72	\$4,939.06	3.2	
23	775	0.47	3045	106868	\$15,922.48	\$5,187.84	3.1	
24	808	0.55	3584	111514	\$16,158.24	\$5,432.66	3.0	
25	842	0.64	4183	116161	\$16,394.00	\$5,673.84	2.9	
26	876	0.74	4854	120807	\$16,629.76	\$5,910.81	2.8	
27	909	0.86	5609	125454	\$16,865.53	\$6,142.76	2.7	
28	943	0.99	6437	130100	\$17,101.29	\$6,370.29	2.7	
29	977	1.13	7353	134746	\$17,337.05	\$6,592.64	2.6	
30	1010	1.28	8372	139393	\$17,572.81	\$6,808.82	2.6	

Pipe Material Properties		Location			Fluid Properties				
Material:	Copper	<b>Houston, TX</b>			k (W/(m <sup>2</sup> C)):	0.606			
Notes:	CS12200 - Type K				Latitude (°):	29.97	ρ (kg/m <sup>3</sup> ):	1000	
Inner Diameter (in):	0.745				Longitude (°):	95.28	c <sub>p</sub> (J/(kg°C)):	4181	
Outer Diameter (in):	0.875				Timezone:	6	Inlet fluid temperature (°C):	20	
Bend Coefficient, Kb:	0.4				Electricity Rate (\$/kWh):	\$0.05960	Outlet tolerance (°C):	1	
Maximum Run Length (m):	50						Viscosity ((N*sec)/m <sup>2</sup> ):	0.00089	
Efficiencies		Depth			Costs				
Pump (%):	100.0%	<b>150 mm</b>			Pipe (\$/m):	\$7.00			
Pavement to Fluid (%):	100.0%				Maintenance (\$/yr):	\$1,000.00			
Extra pipe length (m):	0.0%				Other Capital Cost (\$):	\$10,500.00			
Flowrate (L/min)	Network Length (m)	Pump Power (hp)	Grid Consumption (kWh)	Energy Harnessed (kWh)	Initial Cost	Yearly Savings	Payback Period (years)		
1	33	0.00	0	4520	\$10,731.77	\$730.60	14.7		
2	66	0.00	0	9040	\$10,963.54	\$461.21	23.8		
3	99	0.00	1	13561	\$11,195.30	\$191.87	58.3		
4	132	0.00	4	18081	\$11,427.07	\$77.37	147.7		
5	166	0.00	10	22601	\$11,658.84	\$346.43	33.7		
6	199	0.00	20	27121	\$11,890.61	\$615.26	19.3		
7	232	0.01	35	31642	\$12,122.38	\$883.73	13.7		
8	265	0.01	58	36162	\$12,354.15	\$1,151.77	10.7		
9	298	0.01	91	40682	\$12,585.91	\$1,419.25	8.9		
10	331	0.02	135	45202	\$12,817.68	\$1,686.01	7.6		
11	364	0.03	193	49723	\$13,049.45	\$1,951.97	6.7		
12	397	0.04	267	54243	\$13,281.22	\$2,216.95	6.0		
13	430	0.06	361	58763	\$13,512.99	\$2,480.73	5.4		
14	464	0.07	477	63283	\$13,744.75	\$2,743.25	5.0		
15	497	0.09	618	67804	\$13,976.52	\$3,004.28	4.7		
16	530	0.12	754	72324	\$14,208.29	\$3,265.59	4.4		
17	563	0.15	948	76844	\$14,440.06	\$3,523.39	4.1		
18	596	0.18	1178	81364	\$14,671.83	\$3,779.11	3.9		
19	629	0.22	1449	85884	\$14,903.60	\$4,032.38	3.7		
20	662	0.27	1760	90405	\$15,135.36	\$4,283.26	3.5		
21	695	0.32	2117	94925	\$15,367.13	\$4,531.35	3.4		
22	728	0.39	2530	99445	\$15,598.90	\$4,776.16	3.3		
23	762	0.46	2994	103965	\$15,830.67	\$5,017.90	3.2		
24	795	0.54	3518	108486	\$16,062.44	\$5,256.06	3.1		
25	828	0.63	4113	113006	\$16,294.20	\$5,489.99	3.0		
26	861	0.73	4773	117526	\$16,525.97	\$5,720.10	2.9		
27	894	0.84	5507	122046	\$16,757.74	\$5,945.76	2.8		
28	927	0.97	6330	126567	\$16,989.51	\$6,166.12	2.8		
29	960	1.11	7230	131087	\$17,221.28	\$6,381.86	2.7		
30	993	1.26	8221	135607	\$17,453.04	\$6,592.19	2.6		

## Appendix B: Study One: Constant vs. Varying Poisson's Ratio

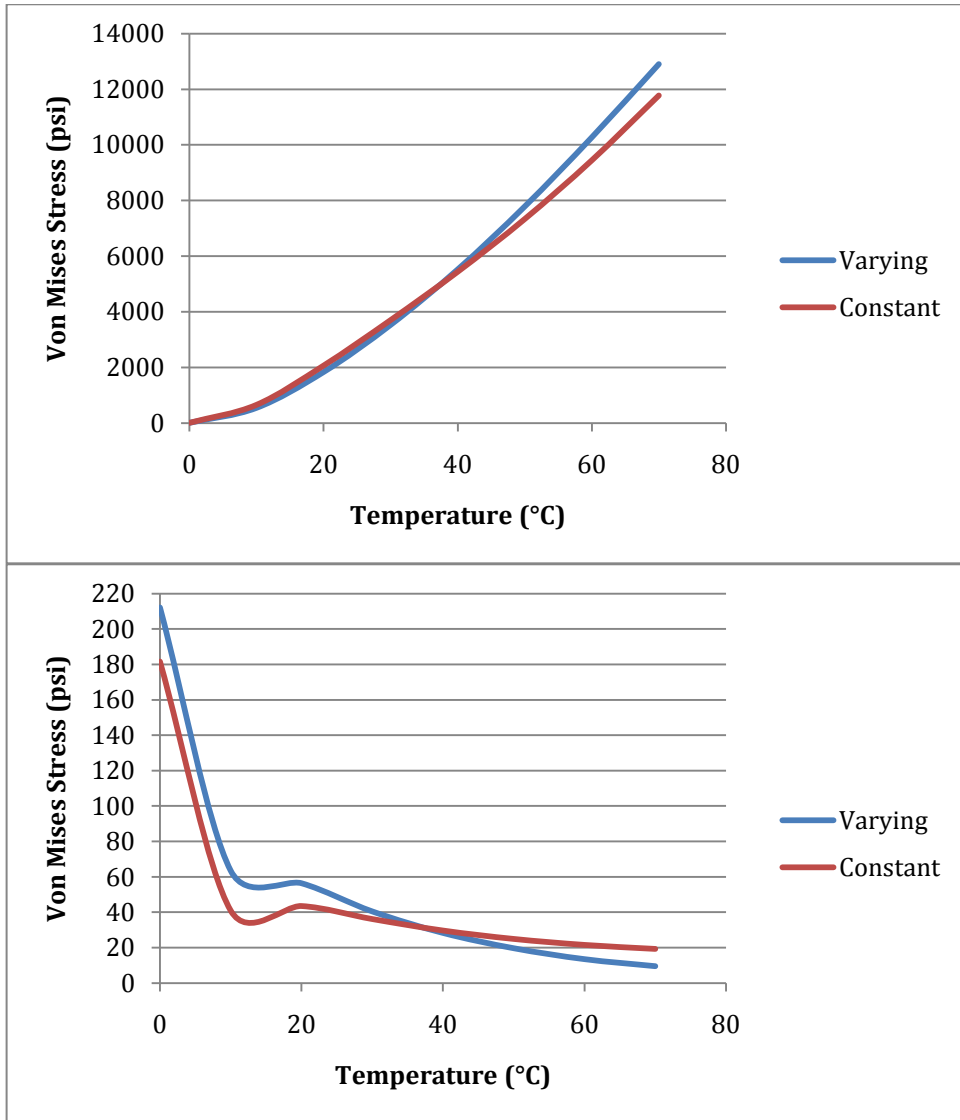


Figure 24: Constant vs. varying Poisson's Ratio (2" pipe depth) (top) copper pipe (bottom) HMA

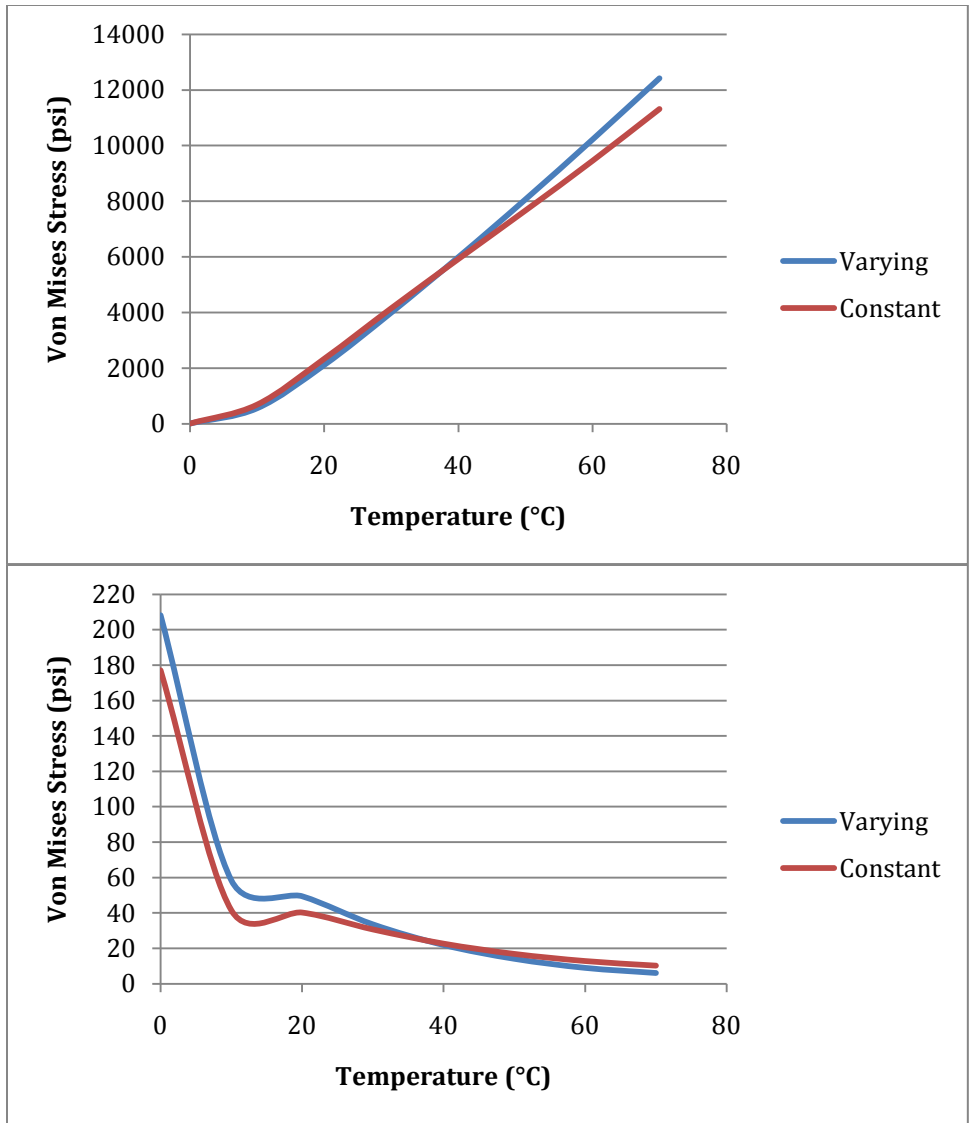


Figure 25: Constant vs. varying Poisson's Ratio (4" pipe depth) (top) copper pipe (bottom) HMA

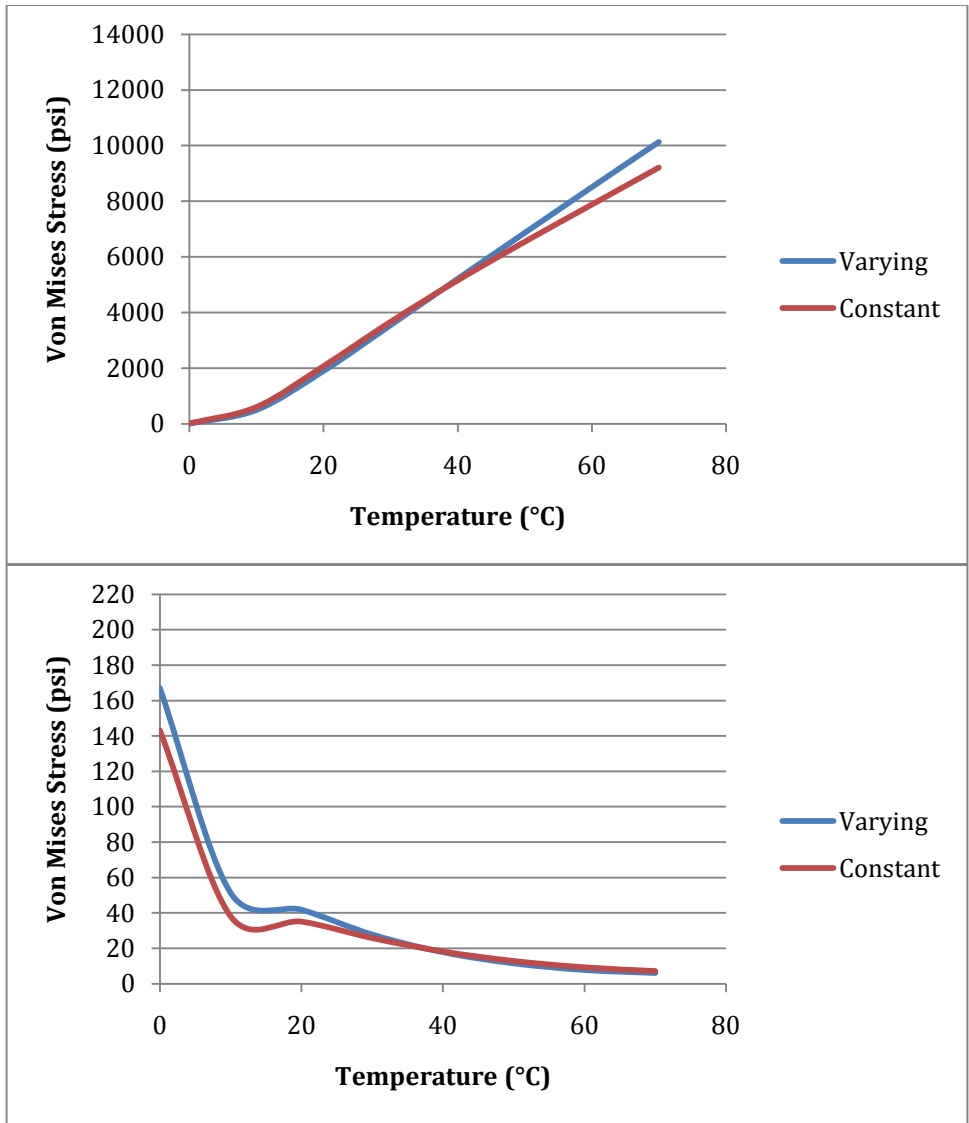


Figure 26: Constant vs. varying Poisson's Ratio (6" pipe depth) (top) copper pipe (bottom) HMA